

NASA Technical Paper 1244

Flight-Measured Buffet  
Characteristics of a Supercritical  
Wing and a Conventional Wing on  
a Variable-Sweep Airplane

Richard C. Monaghan

MAY 1978

**NASA**

NASA Technical Paper 1244

Flight-Measured Buffet  
Characteristics of a Supercritical  
Wing and a Conventional Wing on  
a Variable-Sweep Airplane

Richard C. Monaghan  
*Dryden Flight Research Center*  
*Edwards, California*



National Aeronautics  
and Space Administration

**Scientific and Technical  
Information Office**

1978

FLIGHT-MEASURED BUFFET CHARACTERISTICS OF A SUPERCRITICAL WING  
AND A CONVENTIONAL WING ON A VARIABLE-SWEEP AIRPLANE

Richard C. Monaghan  
Dryden Flight Research Center

INTRODUCTION

Modern fighter aircraft are required to fly at transonic speeds at sustained high angles of attack and elevated load factors. These conditions contribute to a number of control system, aerodynamic, and structural problems. A factor that contributes to these problems is separated airflow over the aircraft, which is detected as buffeting of the airplane structure.

Buffet has been the subject of a number of investigations both in flight and in the wind tunnel. These investigations have shown that buffet characteristics can be improved by the use of deflected leading- and trailing-edge flaps, which can be optimized for maneuver performance by programming flap deflections to Mach number and angle-of-attack conditions (refs. 1 and 2); the addition of strakes forward of the wing to produce vortex flow over the wing and thus keep the flow in the influenced areas from separating (ref. 2); and the use of new airfoil sections, specifically those referred to as supercritical sections (refs. 3 and 4).

Previous flight tests of a supercritical airfoil section designed for a transport aircraft application had indicated an improvement in the transonic buffet characteristics and suggested the possibility of an even greater improvement for a highly maneuverable aircraft (refs. 3 and 4). With this in mind and as part of the transonic aircraft technology (TACT) program, the F-111 TACT aircraft was designed with a supercritical airfoil section. The design objective was to maximize the transonic maneuver performance without degrading cruise performance.

The F-111 TACT aircraft is capable of maneuvering at high angles of attack ( $16^\circ$  to  $18^\circ$ ). The swing-wing design enabled the evaluation of nonoptimum supercritical flow wing sweep configurations, and the availability of data on this same aircraft with a conventional F-111A wing enabled a comparison with a similar aircraft.

Presented in this report are data from the F-111A and F-111 TACT aircraft obtained from windup-turn maneuvers performed at wing sweep angles of 26°, 35°, and 58° for a Mach number range of 0.60 to 0.95. On the F-111 TACT aircraft, the supercritical wing was designed to achieve optimum supercritical flow when operating at a wing sweep angle of 26°. The F-111 TACT data presented for wing sweep angles of 35° and 58° represent off-design conditions.

Buffet intensity, buffet intensity rise, and flight-measured wing pressure data are presented. Wind tunnel oil-flow photographs from the F-111 TACT aircraft model are used to help interpret flight data. Flight and wind tunnel data for the two aircraft are compared to illustrate trends in buffet intensity and buffet intensity rise.

### SYMBOLS AND ABBREVIATIONS

Physical quantities in this report are given in the International System of Units (SI) and parenthetically in U.S. Customary Units. The measurements were taken and the calculations were made in U.S. Customary Units. Factors relating the two systems are presented in reference 5.

|              |  |
|--------------|--|
| $a_{n_{cg}}$ | normal acceleration at airplane center of gravity, g             |
| $a_{n_{cp}}$ | normal acceleration at cockpit, g                                |
| $a_{n_{wt}}$ | normal acceleration at wingtip, g                                |
| $B_w$        | wing bending moment at wing strain-gage location, m-N<br>(ft-lb) |
| BIR          | buffet intensity rise  |
| $C_{N_A}$    | airplane normal-force coefficient, $\frac{a_{n_{cg}} W}{qS}$     |
| $C_p$        | local pressure coefficient                                       |
| M            | Mach number  |
| q            | free-stream dynamic pressure, $N/m^2$ (lb/ft <sup>2</sup> )      |
| rms          | root mean square   |
| S            | wing reference area, m <sup>2</sup> (ft <sup>2</sup> )           |

|           |  |
|-----------|--|
| $T_w$     | wing torsion at wing strain-gage location, m-N (ft-lb) |
| $W$       | airplane mass, kg (lb)                                 |
| $x/c$     | local wing chord location, percent aft of leading edge |
| $\alpha$  | airplane true angle of attack, deg                     |
| $\lambda$ | wing sweep angle, deg                                  |
| $\sigma$  | root mean square of associated quantity                |
| $\Phi$    | power spectral density of associated quantity          |

### AIRPLANE DESCRIPTION

The F-111A and F-111 TACT aircraft are shown in figure 1. Throughout this report these aircraft are referred to as the baseline and TACT aircraft, respectively.

The TACT aircraft is a modification of the baseline aircraft, F-111A airplane number 13. The modification consists of a new wing having a supercritical airfoil section and a different wing planform, a new overwing fairing, and a new fixed leading-edge glove. The wing geometry for the two aircraft is illustrated in figure 2, and physical characteristics of the wings are given in table 1.

The baseline and TACT aircraft have wings of similar construction, incorporating a primary structural wing box with milled stressed skins and multiweb construction. Both aircraft have leading- and trailing-edge high-lift devices attached to the wing box. These high-lift devices are designed for takeoff and landing only. Both wing airfoils are approximately 10.5-percent thick near the pivot; at the tip, the baseline wing is 9.8-percent thick and the TACT wing is 5.4-percent thick. One of the primary features of aircraft of the F-111 series is their ability to change wing sweep angle during flight.

For both aircraft, power is provided by two TF30-P-3 axial flow, dual-compressor turbofan engines with afterburners. The empennage consists of a fixed vertical stabilizer with rudder for directional control and all-movable horizontal stabilizers that move symmetrically for pitch control and differentially for roll control. Wing spoilers augment roll control for pilot stick inputs in excess of one-half maximum travel. For the baseline aircraft, the spoilers are deactivated for wing sweep angles greater than 45°. Fuel can be carried in both the fuselage and wings for the baseline aircraft and only in the fuselage for the TACT aircraft. However, all data were taken with the wing tanks empty. The design masses for the baseline and TACT aircraft were 33,100 kilograms (73,000 pounds) and 31,750 kilograms (70,000 pounds), respectively.

## INSTRUMENTATION AND RECORDING

The following parameters were measured on both test aircraft: Mach number, pressure altitude, airplane angle of attack, wingtip normal acceleration, wing-root bending moment, normal acceleration at the cockpit, and normal acceleration at the center of gravity. The parameters measured on the TACT aircraft only were wing-root torque and wing pressures.

A nose-boom-mounted air data system (described in ref. 6) was used to measure angle of attack and total and static pressure. Angle of attack was measured relative to the wing reference chord at the pivot for the airplane in the assembly position. This wing reference chord is  $1^\circ$  leading edge up from the fuselage reference line.

Wing bending moment and torque were measured by using semiconductor strain gages (ref. 7), which for equivalent loads produce much higher gage outputs than conventional strain gages. The outputs of the wingtip accelerometer and wing bending-moment and torque gages were high-pass filtered at 2.5 hertz to eliminate gage response due to maneuver loads. The recording system acted as a filter above 40 hertz. These filters, used in conjunction with the wingtip accelerometers and the wing bending and torque gages, produced data of greater resolution in the range of the frequencies of interest than instrumentation without filters. The cockpit and center-of-gravity accelerometers were mounted on major structural members near the pilot's seat and near the airplane's center of gravity, respectively.

The right wing of the TACT airplane was instrumented with 162 pressure ports. The 45 ports used for this study were located in three rows on the wing outboard upper surface, as shown in figure 2. Each pressure port was connected to its own pressure transducer with a maximum line length of 1.53 meters (5 feet) between port and transducer. This system allowed accurate pressure measurements during maneuvering flight.

Data were acquired using a pulse code modulation system. The data were stored on an onboard tape recorder and also were telemetered to a ground station tape recorder. Selected telemetry data were displayed for real-time review. The onboard recorder was the primary source of information for this report.

The errors in the unsteady flow response parameters associated with the instrumentation and recording system were considered negligible with respect to the data scatter. The angle of attack was corrected for upwash and had an accuracy of  $\pm 0.25^\circ$ . The normal-force coefficient had an accuracy of approximately  $\pm 0.03$ .

## FLIGHT TEST CONDITIONS

The baseline and TACT aircraft were tested at three common wing sweep angles— $26^\circ$ ,  $35^\circ$ , and  $58^\circ$  ( $58^\circ$  being the maximum attainable sweep angle on the TACT aircraft). At each wing sweep angle, data were gathered for a Mach number

range of 0.60 to 0.95. All data were obtained from 10- to 30-second windup-turn maneuvers with no fuel in the wings and at a dynamic pressure of  $14,400 \pm 2400 \text{ N/m}^2$  ( $300 \pm 50 \text{ lb/ft}^2$ ). For the portions of the windup-turn maneuvers at the higher angles of attack where available power was insufficient to maintain constant flight conditions, altitude was sacrificed to maintain Mach number.

## DATA INTERPRETATION AND ANALYSIS

Figure 3 presents typical data obtained from several strain gages and accelerometers and illustrates the TACT aircraft's structural response to buffeting. Figure 4 shows the frequency response for each of the buffet sensors on the TACT aircraft in the form of power spectral density. These power spectral density plots represent short data segments (512 points over a period of 2.5 seconds) taken during maneuvers similar to the maneuver for which data are shown in figure 3. The power spectral density data were high-pass filtered with a third-order filter having a break frequency of 2.5 cycles per second, and were smoothed using a 7-point Hann-Tukey window. Each instrument responded according to its type and location. The frequencies indicated in figure 4 were selected from those listed in reference 8. The normal accelerometers at the pilot's seat and at the center of gravity respond to a frequency near that of the first wing torsion mode. The frequency for the first wing torsion mode is also indicated as a possible second vertical fuselage bending frequency in reference 8. The cockpit accelerometer also responds to a number of other wing frequencies that indicate substantial output. For some flight conditions other than the condition illustrated in figure 3, the center-of-gravity accelerometer responds to a second frequency which corresponds to that of the first wing bending mode. The wing-root bending strain gage and torque strain gage respond almost exclusively to the first symmetric wing bending and first wing torsion frequencies, respectively. The wingtip accelerometer responds to a number of frequencies, primarily those of the first symmetric wing bending and first wing torsion modes.

Buffet intensity data were calculated as the root mean square (rms) value of the dynamic response of the individual accelerometer or strain-gage output. Figure 5 presents the responses of the strain gages and accelerometers to a typical windup-turn maneuver for the TACT aircraft. All the sensors indicate similar trends. The data from the wingtip accelerometers consistently have the least scatter and best repeatability and, therefore, are used in this report as the primary indicator of buffet response. The ratio of the rms value of the wingtip accelerometer to the rms value of the accelerations measured at the cockpit and center of gravity, and the torque and bending moment measured inboard on the wing remain approximately the same as those indicated in figure 5 at all wing sweeps and Mach numbers. Similar comparisons of buffet parameters on the baseline aircraft also indicate the wingtip accelerometer to be the most consistent source of buffet information.

The buffet intensity rise (BIR) point is defined for this report as the first increase in buffet intensity as measured by the wingtip accelerometer and was selected from time history plots (fig. 3) and from curves of  $\sigma_{a_{n_{wt}}}$  as a function of

$C_{N_A}$ . This definition is similar to definitions used for buffet onset in previous reports. The BIR point as selected in this report corresponds to the pilot's evaluation of when the buffet intensity he felt increased from none or light intensity to moderate intensity. The BIR points also correspond closely to a magnitude of 0.5g rms measured by the wingtip accelerometer. On the TACT aircraft, a level of buffet intensity characterized by the pilot as light exists before the BIR point at the higher transonic Mach numbers. This low intensity level could be significant in applications to commercial aviation.

Wind tunnel data in the form of upper-surface oil-flow photographs are also presented for comparison with in-flight upper-surface pressure measurements. The wind tunnel model was a 1/6-scale semispan model configured to the cruise design point of Mach 0.85 and a model dynamic pressure of 20,300 N/m<sup>2</sup> (424 lb/ft<sup>2</sup>). The model is of steel and is considered rigid for all practical purposes.

## RESULTS AND DISCUSSION

The aircraft buffet characteristics discussed in this report are considered to be a response to wing flow separation caused by wing shocks or boundary layer separation, or both. This assumption is considered valid because the primary source of buffet intensity data, the wingtip accelerometer, is remote from other sources of vibration, and power spectral density plots of the wingtip accelerometer data (fig. 4) show little power except at the wing mode frequencies.

### Buffet Response

BIR boundaries and buffet intensity curves are presented for the TACT and baseline aircraft for wing sweep angles of 26°, 35°, and 58°. The data are presented for a Mach number range of 0.60 to 0.95.

Buffet intensity rise boundary. - The BIR boundaries for the TACT and baseline aircraft are presented in figure 6 in the form of  $C_{N_A}$  as a function of Mach number. The symbols represent flight data, and the solid line is a fairing of the flight data. The fairing was determined primarily by using the rms buffet intensity data for a dynamic pressure of 14,400 N/m<sup>2</sup> (300 lb/ft<sup>2</sup>) to determine the magnitude and the remaining flight data (that is, time histories and rms buffet intensity data for other dynamic pressures) to aid in the determination of the shape of the fairing. The dashed line in figure 6(b) represents data from an earlier study on an F-111A aircraft (ref. 9). These data were analyzed using time history plots similar to those used to determine the data represented by the square symbols in the figure, and the two sets of data agree reasonably well. The broken lines represent 1g flight at the TACT design mass of 31,750 kilograms (70,000 pounds) and at the altitudes indicated. These 1g lines are used to compare the flight cruise altitude capabilities of the two aircraft when operating below the BIR boundary.

At a wing sweep angle of  $26^\circ$ , the TACT BIR boundary (fig. 6(a)) is characterized by a slowly increasing  $C_{N_A}$  value as Mach number increases from 0.60 to 0.92. For Mach numbers between 0.92 and 0.94, the  $C_{N_A}$  for the BIR boundary increases abruptly. Data are not available above Mach 0.94 due to the Mach number/wing sweep limitations of the aircraft.

The BIR boundary characteristics of the baseline aircraft at the same wing sweep angle are quite different (fig. 6(b)). For Mach numbers below 0.75, the data for the baseline aircraft indicate a relatively constant BIR boundary. At Mach numbers between 0.75 and 0.85, the  $C_{N_A}$  value for the BIR boundary decreases at a rapidly increasing rate. At Mach numbers above 0.85, the BIR boundary remains relatively constant at a low value of  $C_{N_A}$ .

BIR boundaries for wing sweep angles of  $35^\circ$  and  $58^\circ$  are shown in figures 6(c) to 6(f). For each aircraft, the trends in the data for a wing sweep angle of  $35^\circ$  are quite similar to those for a wing sweep angle of  $26^\circ$ . The trends in the data for a wing sweep angle of  $58^\circ$  indicate a considerably different BIR boundary than for the lesser wing sweep angles. This difference is probably due to leading-edge separation and the formation of a leading-edge vortex (ref. 10), which influences the flow on both aircraft and causes the buffet characteristics of the aircraft to be similar.

The BIR boundary indicates that for the baseline aircraft the wing must be swept from  $26^\circ$  to  $35^\circ$  at a Mach number of 0.75 and to  $58^\circ$  for Mach numbers from 0.85 to 0.95 to achieve a high normal-force coefficient before the BIR. For the TACT aircraft, a wing sweep angle of  $26^\circ$  may be maintained throughout the transonic speed range. The wing sweep angles selected to maintain a high normal-force coefficient before the BIR are not necessarily those that would be selected to achieve the best lift or drag performance. Information relating to these two performance areas is given in reference 11.

From Mach 0.60 to 0.75, the TACT and baseline aircraft maintain relatively similar  $C_{N_A}$  values for the BIR boundary. Above Mach 0.75, the baseline BIR boundary begins to decrease rapidly, whereas the TACT BIR boundary steadily increases, which, as Mach number increases, results in a much higher  $C_{N_A}$  value for the BIR boundary on the TACT aircraft than on the baseline aircraft. The intersection of the BIR boundary with the constant altitude 1g lines in figure 6 indicates that the TACT aircraft, at the higher Mach numbers presented, is capable of flying at much greater altitudes than the baseline aircraft without exceeding the BIR boundary.

The improvements in the BIR boundary characteristics of the TACT aircraft over those of the baseline aircraft at the higher transonic Mach numbers are the result of an aft shock location on the supercritical wing. Shock locations, shock movements, and flow separation on the TACT aircraft are discussed later in this report.

Buffet intensity. - Buffet intensity data for the TACT and baseline aircraft are presented in figure 7 in the form of the rms wingtip acceleration as a function of angle of attack. The data indicate the effects of Mach number and wing sweep on the buffet intensity characteristics. The data points in each curve are from a single flight maneuver and were generally verified by data from one or more duplicate maneuvers which are not shown in this report.

The evaluation of the buffet intensity curves presented in figure 7 is important not only for the selection of the BIR point, but also for the determination of buffet intensity levels and rates of increase in intensity. For example, at a wing sweep angle of  $26^\circ$  (fig. 7(a)), the TACT aircraft has a noticeably higher buffet intensity level at angles of attack below the BIR point for Mach 0.94 than for the low Mach numbers. The pilot reported this buffet intensity as light. After the BIR point in the Mach 0.94 curve, the buffet intensity rises slowly until a second buffet intensity rise point occurs. After the second buffet intensity rise point, the intensity rises relatively rapidly. At Mach numbers of 0.89 and above, the buffet intensity curves have similar trends, but for Mach numbers from 0.71 to 0.85, the trends are different. For example, at Mach 0.80 the BIR point occurs at a much lower angle of attack than at Mach 0.94, and the rise in buffet intensity is very rapid immediately after the BIR point. This change in buffet intensity characteristics is due to the change in the flow over the wing that takes place between these two speed ranges and is discussed in a later section.

For the baseline aircraft at a wing sweep angle of  $26^\circ$  (fig. 7(b)) and for Mach numbers of 0.85 and above, the data indicate that the BIR point occurs at a low angle of attack. The buffet intensity rises to a level that the pilot reported as moderate and then remains at this constant level until a second buffet intensity rise takes place. For Mach numbers of 0.73 and 0.82, only one buffet intensity rise is indicated.

Figure 8 presents  $C_{N_A}$  as a function of angle of attack. The flight conditions for these data correspond to those for the data presented in figure 7. The breaks and trends in the  $C_{N_A}$  curves correspond closely to the characteristics of the buffet intensity curves.

#### TACT Wing Flow Characteristics

Changes in buffet intensity levels largely reflect changes in wing upper-surface flow conditions. Figures 9 and 10 present flight-measured upper-surface pressure distributions and wind tunnel oil-flow photographs, respectively, obtained for the TACT aircraft at a wing sweep angle of  $26^\circ$ . The data shown in these figures are for the same Mach numbers as the buffet intensity data presented in figure 7(a). Figure 9 presents the chordwise pressures at 60-percent, 76-percent, and 92-percent wing semispan (orifice rows C, B, and A, respectively) for a range of angles of attack above and below the BIR point. The data for each orifice row are divided into two plots according to angle of attack to make the curves more definable.

The pressures at 60-percent and 76-percent wing semispan are representative of the flow over the majority of the wing and are the object of the following discussion unless otherwise stated.

The oil-flow photographs presented in figure 10 are from a 1/6-scale semispan model. The chordwise lines on the wing correspond to the orifice rows for the flight-measured wing pressures presented in figure 9. The flight measurements were made on the right wings, whereas the wind tunnel oil-flow photographs were taken on a left wing semispan model. The spanwise straight lines on the model wing at 5-percent and 70-percent wing chord are the oil dispensing lines.

At Mach 0.70 (fig. 9(a)), strong expansion and recompression occur close to the leading edge. The recompression moves slightly rearward on the wing as angle of attack increases to  $8^\circ$ , then forward again for angles of attack of  $9^\circ$  and above. The flight-measured upper-surface pressures indicate the formation of a separation bubble behind the recompression for angles of attack of  $8^\circ$  and above at wing orifice row C and for  $9^\circ$  and above at row B. This separated region tends to grow with further increases in angle of attack.

The data at this Mach number also show that as angle of attack increases, the trailing-edge boundary layer thickens, as evidenced by the reduction in the second velocity peak near the trailing edge. The decreasing trailing-edge pressures also indicate that the trailing-edge boundary layer thickens to the point of separation as angle of attack approaches  $9^\circ$ .

The BIR point occurs at an angle of attack of  $8^\circ$ , which corresponds to the first indication of a separated region behind the leading-edge recompression. Apparently, the growth of the separation bubble on the forward part of the wing and the spread of the trailing-edge separation forward on the wing give rise to the steadily increasing buffet intensity measured by the wingtip accelerometer (fig. 7).

The wind tunnel oil-flow photographs (fig. 10(a)) agree with the flight pressures as regards the movement of the leading-edge recompression with angle of attack. However, the oil flow at this Mach number is not sufficiently detailed to define the regions of separated flow.

At Mach 0.85 (fig. 9(b)), a wing shock forms well back on the wing, as far back as the 60-percent wing chord for an angle of attack of  $8^\circ$ . The pressures for angles of attack of  $8^\circ$  and below recover at the trailing edge, and there appear to be no large areas of separation. The pressures for angles of attack of  $9^\circ$  and above indicate that the shock has moved forward and the trailing-edge pressures have decreased rapidly. These changes, in addition to the small change in pressure from the shock to the trailing edge, indicate that the flow is separated from the shock location to the trailing edge.

Figure 7(a) shows that at an angle of attack between  $8^\circ$  and  $9^\circ$ , the buffet intensity begins to rise at a relatively high rate. This rise appears to be related to the sudden forward movement of the wing shock and is accompanied by a large chordwise area of separated flow.

The wind tunnel oil-flow photographs (fig. 10(b)) indicate no large areas of separated flow for angles of attack of  $8^\circ$  and below, and the indications of shock location and movement are similar to those for the flight pressures. Oil-flow photographs are not available for an angle of attack of  $9^\circ$ , but those shown for angles of attack of  $10^\circ$  and  $12^\circ$  indicate a large area of spanwise and reverse flow, indicative of separation, extending from the shock location to the trailing edge.

At Mach 0.95, the pilot reported light buffet at angles of attack up to approximately  $11^\circ$ . It is not clear from the chordwise pressure distributions of figure 9(c) how much separated flow existed on the wing at angles of attack below  $11^\circ$ , but some probably existed on the aft part of the wing, especially near the tip, because the upper-surface pressures do not recover well at the trailing edge. For an angle of attack of nearly  $13^\circ$ , the pressure distributions show evidence of a weak shock recompression that begins to move forward, but as before, the extent of the region of separated flow is difficult to interpret from the pressure measurements. The separated flow regions are highly three dimensional, as shown in the oil-flow photographs of figure 10(c), and this further complicates the interpretation of the pressures. The oil-flow photographs show only a small increase in the area of separated flow at angles of attack between  $9^\circ$  and  $13^\circ$ , which probably causes the gradual increase in buffet intensity shown in figure 7(a). This gradual increase differs from the relatively rapid increase in buffet intensity associated with the forward movement of the shock at Mach 0.85.

#### CONCLUDING REMARKS

Windup-turn maneuvers were performed with a conventional F-111A aircraft (referred to as the baseline aircraft) and with the same aircraft fitted with a supercritical wing (referred to as the F-111 transonic aircraft technology (TACT) aircraft). These tests were designed to determine the buffet characteristics of the two aircraft at subsonic and transonic Mach numbers.

In the transonic speed range, the overall buffet characteristics of the aircraft having a supercritical wing were significantly improved over those of the aircraft having a conventional wing. At subsonic speeds (up to Mach 0.75) or at a wing sweep angle of  $58^\circ$  where the supercritical wing is off design, the two aircraft had similar buffet characteristics.

The flight-measured upper-surface pressure measurements and wind tunnel oil-flow photographs generally supported the characteristics observed in the buffet intensity data.

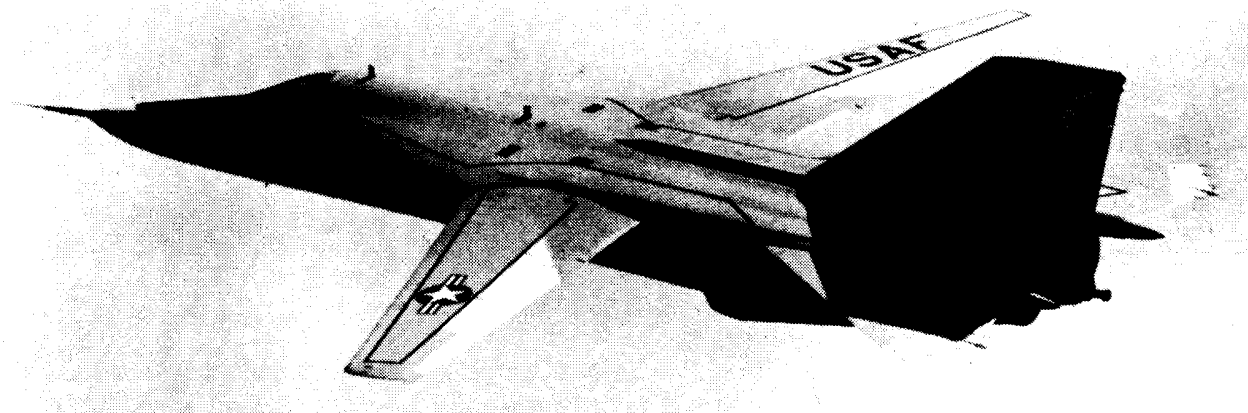
Dryden Flight Research Center  
National Aeronautics and Space Administration  
Edwards, Calif., October 26, 1977

## REFERENCES

1. Monaghan, Richard C.; and Friend, Edward L.: Effects of Flaps on Buffet Characteristics and Wing-Rock Onset of an F-8C Airplane at Subsonic and Transonic Speeds. NASA TM X-2873, 1973.
2. Friend, Edward L.; and Matheny, Neil W.: Preliminary Flight Measurements of the Buffet Characteristics of Prototype Lightweight Fighter Aircraft. NASA TM X-3549, 1977.
3. DeAngelis, V. Michael; and Monaghan, Richard C.: Buffet Characteristics of the F-8 Supercritical Wing Airplane. NASA TM-56049, 1977.
4. DeAngelis, V. Michael; and Banner, Richard D.: Buffet Characteristics of the F-8 Supercritical Wing Airplane. Supercritical Wing Technology—A Progress Report on Flight Evaluations. NASA SP-301, 1972, pp. 85-96.
5. Mechtly, E. A.: The International System of Units—Physical Constants and Conversion Factors. Second Revision. NASA SP-7012, 1973.
6. Sakamoto, Glenn M.: Aerodynamic Characteristics of a Vane Flow Angularity Sensor System Capable of Measuring Flightpath Accelerations for the Mach Number Range From 0.40 to 2.54. NASA TN D-8242, 1976.
7. Davis, Harry J.; and Horn, Leon: Notes on the Use of Semiconductor Strain Gages. TR-1285, Harry Diamond Laboratories, Apr. 30, 1965. (Available from DDC as AD 615802.)
8. Voelker, Leonard S.: Measurement of the Natural Frequencies and Mode Shapes of the TACT Aircraft. AFFDL-TM-74-42-FYS, Air Force Flight Dynamics Lab., Wright-Patterson Air Force Base, Ohio, July 1974.
9. Friend, Edward L.; and Monaghan, Richard C.: Flight Measurements of Buffet Characteristics of the F-111A Variable-Sweep Airplane. NASA TM X-1876, 1969.
10. Hallissy, James B.; and Ayers, Theodore G.: Transonic Wind-Tunnel Investigation of the Maneuver Potential of the NASA Supercritical Wing Concept. Phase I. NASA TM X-3534, 1977.
11. Cooper, James M., Jr.; Hughes, Donald L.; and Rawlings, Kenneth III: Transonic Aircraft Technology - Flight-Derived Lift and Drag Characteristics. Volumes I and II. AFFTC-TR-77-12, Air Force Flight Test Center, Edwards Air Force Base, Calif., July 1977.

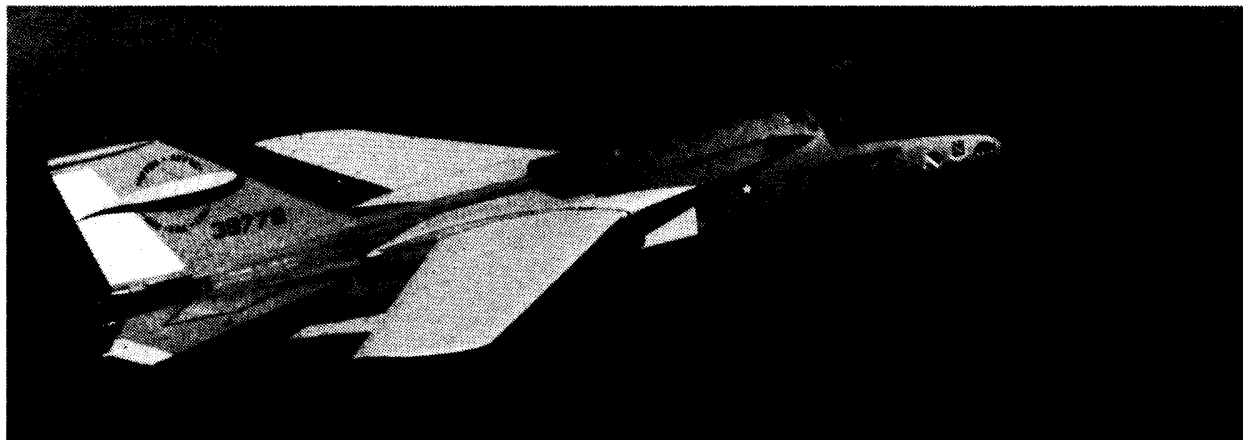
TABLE 1.—PHYSICAL CHARACTERISTICS OF BASELINE AND TACT WINGS

| Wing parameter                                    | Baseline aircraft         | TACT aircraft              |
|---|---------------------------|----------------------------|
| Span (at $\lambda = 16^\circ$ ), m (ft) . . . . . | 19.2 (63.0)               | 18.1 (59.3)                |
| Area, m <sup>2</sup> (ft <sup>2</sup> ) . . . . . | 48.8 (525)                | 56.1 (604)                 |
| Airfoil section—                                  |                           |                            |
| At pivot . . . . .                                | NACA 64A210.68 (modified) | -----                      |
| At butt line 2.36 m (93 in.) . . . .              | -----                     | 9.89-percent supercritical |
| At tip . . . . .                                  | NACA 64A209.8 (modified)  | 5.35-percent supercritical |
| Mean aerodynamic chord, m (in.) . . . . .         | 2.75 (108.5)              | 3.20 (125.5)               |



ECN 2091

(a) F-111A (baseline) aircraft.



ECN 3959

(b) F-111 TACT aircraft.

Figure 1. Test aircraft.

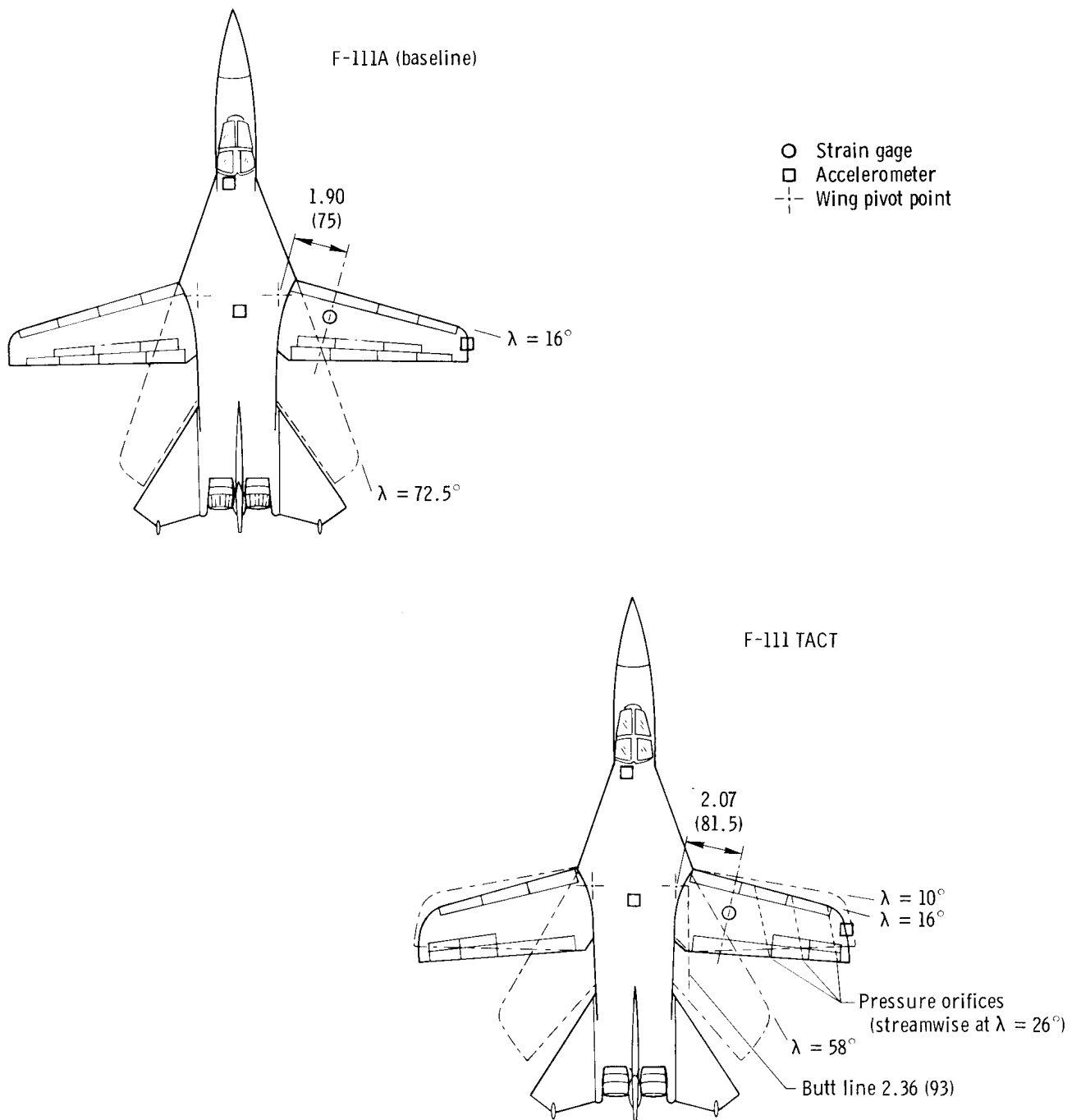


Figure 2. Wing geometry and instrumentation locations for baseline and TACT aircraft. Dimensions are in meters (inches).

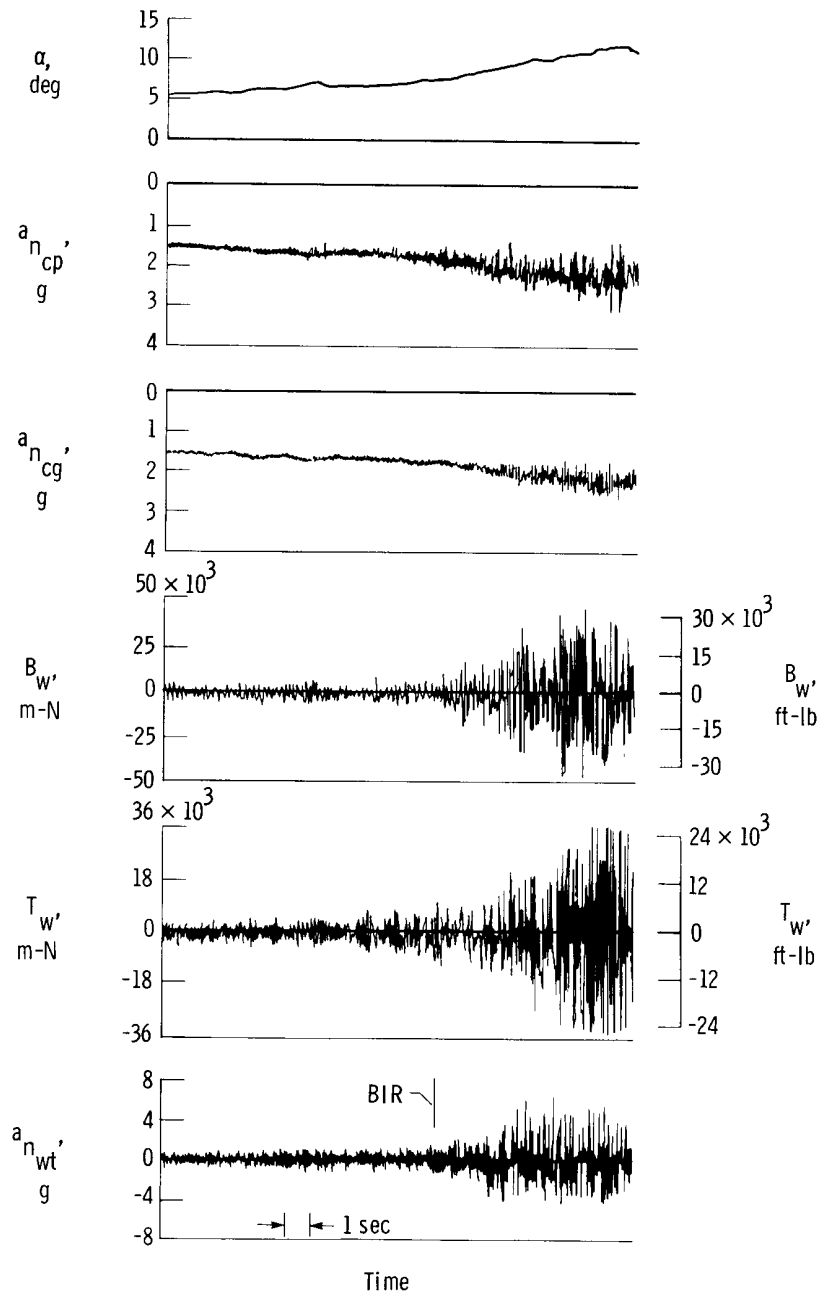


Figure 3. Typical time history of buffet instrumentation on TACT aircraft. Mach 0.90,  $\lambda = 26^\circ$ .

- A First symmetric wing bending mode
- B First antisymmetric wing bending mode
- C First wing torsion mode
- D Second right wing torsion mode

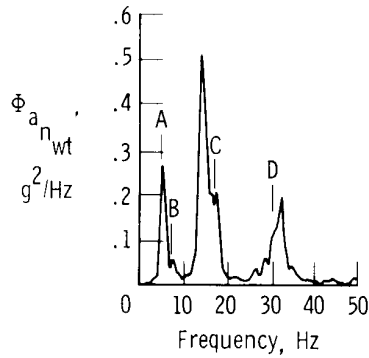
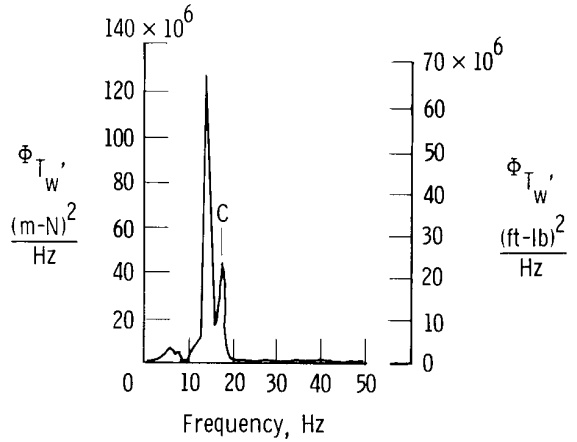
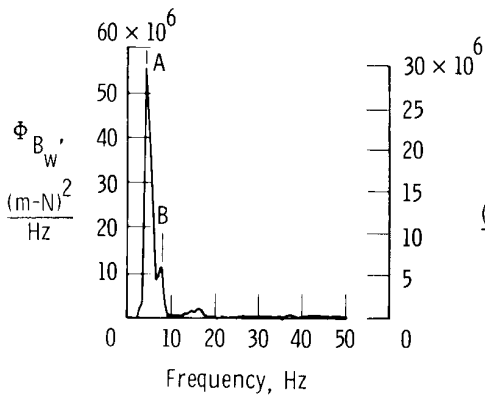
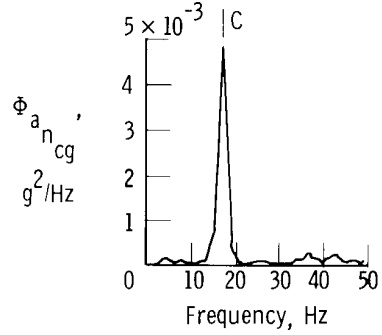
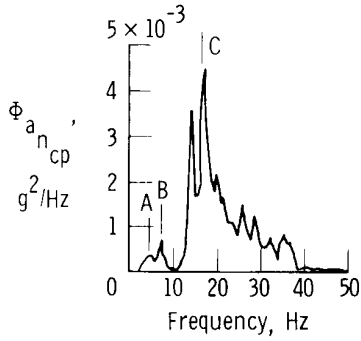


Figure 4. Typical frequency response (power spectral density) of buffet instrumentation on TACT aircraft. Mach 0.81,  $\lambda = 26^\circ$ ,  $\alpha = 10^\circ$ .

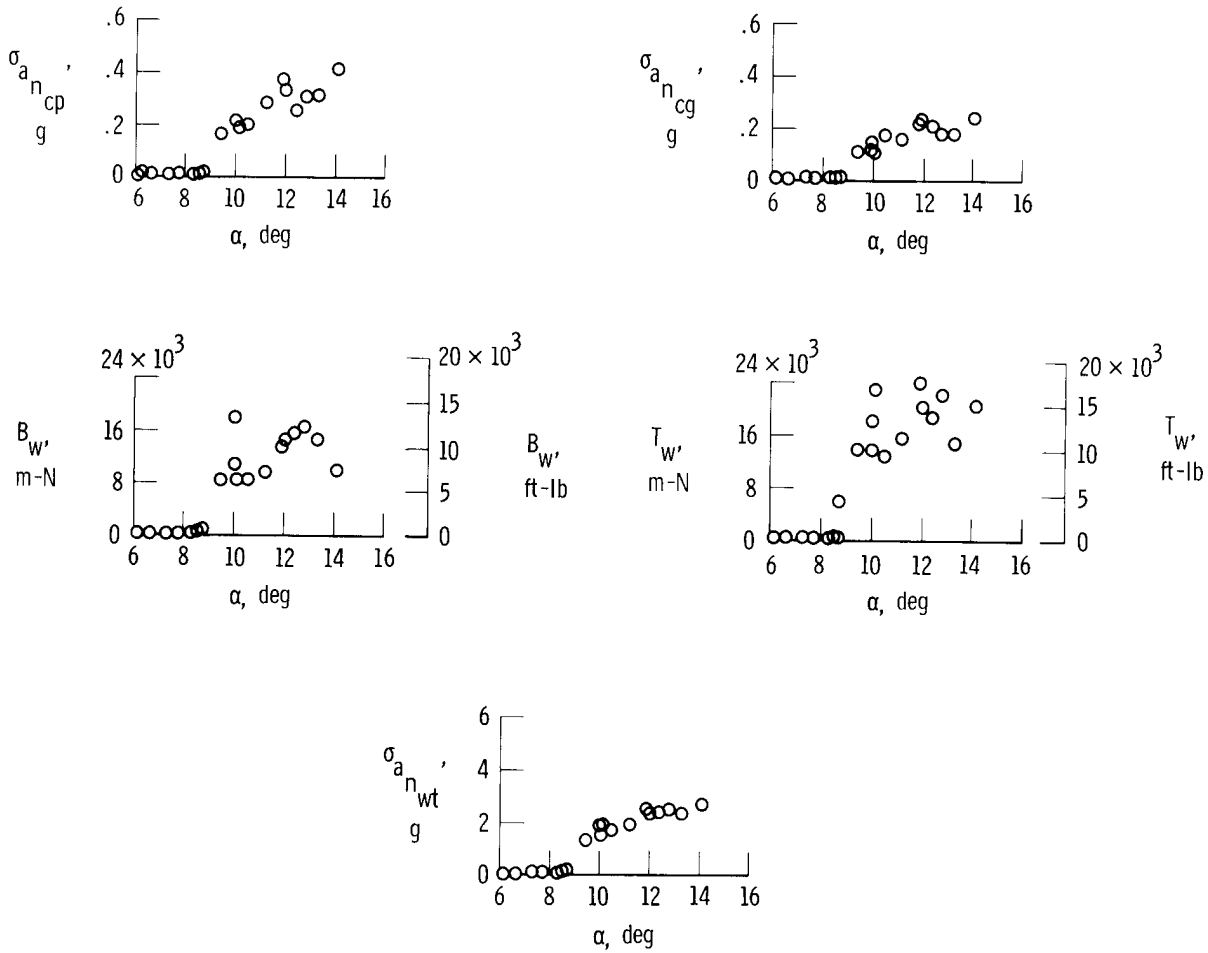
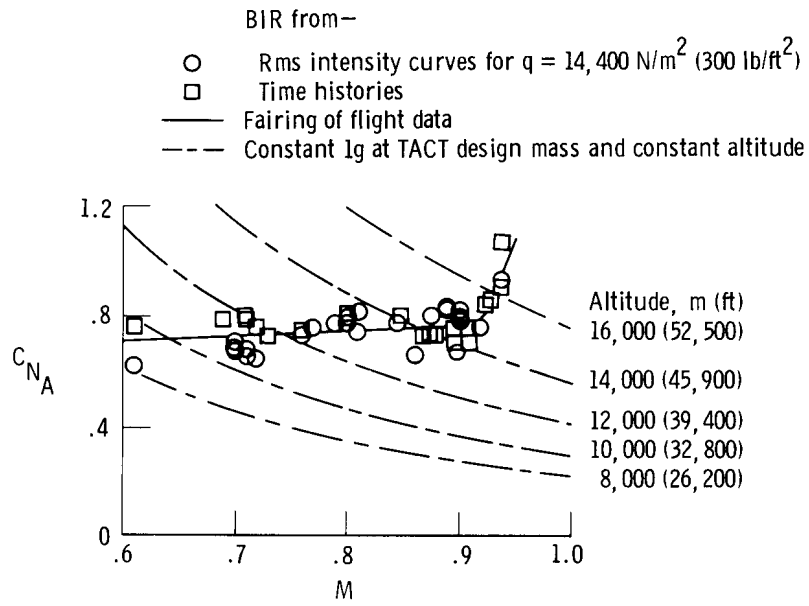
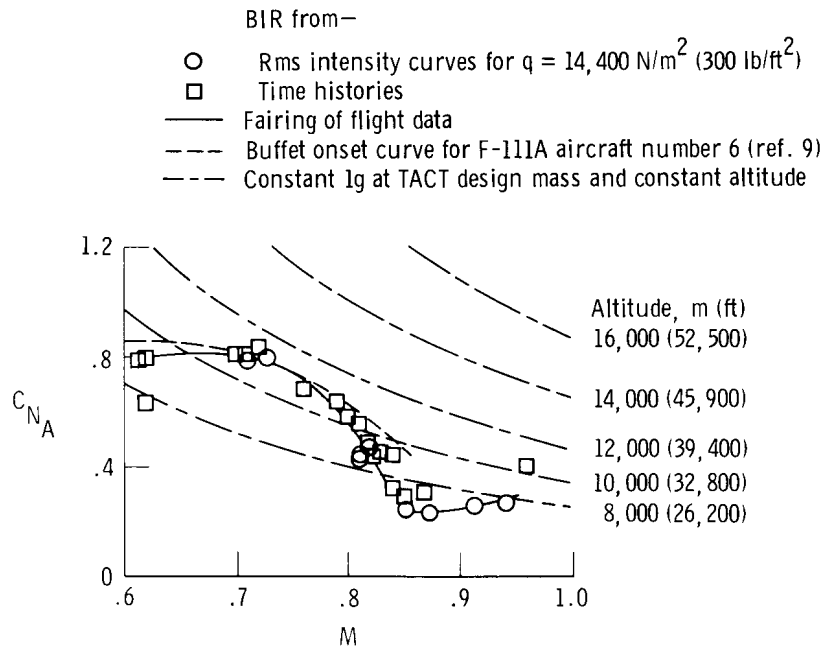


Figure 5. Typical buffet intensity responses of various buffet instrumentation on the TACT aircraft. Mach 0.81,  $\lambda = 26^\circ$ .

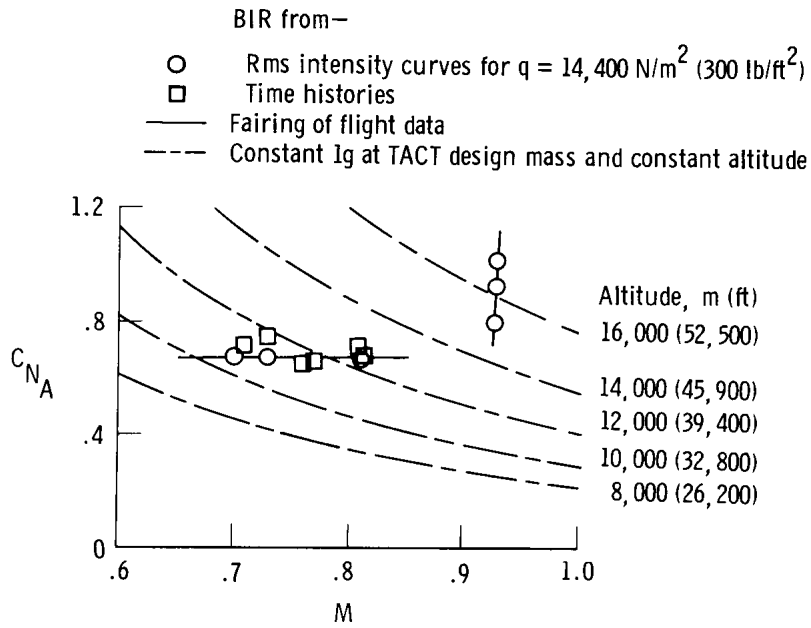


(a) TACT aircraft,  $\lambda = 26^\circ$ .

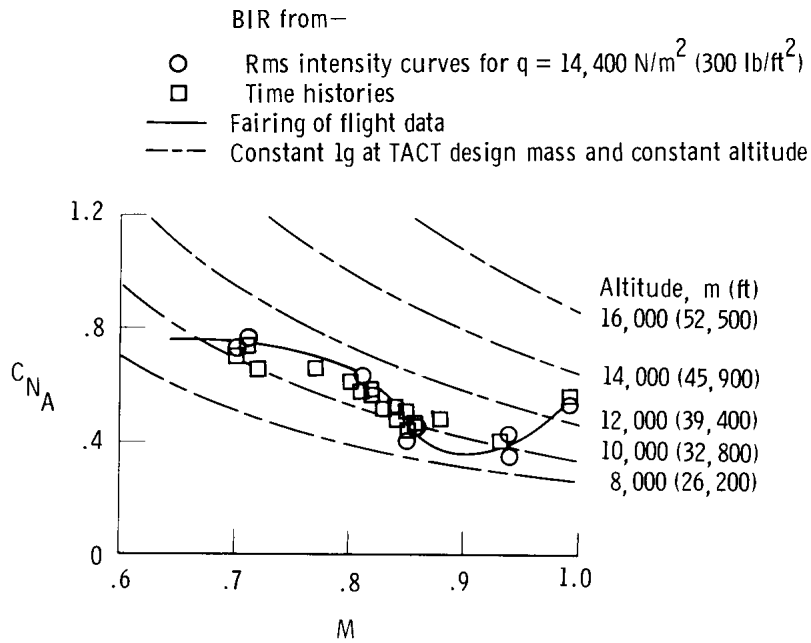


(b) Baseline aircraft,  $\lambda = 26^\circ$ .

Figure 6. BIR boundary.

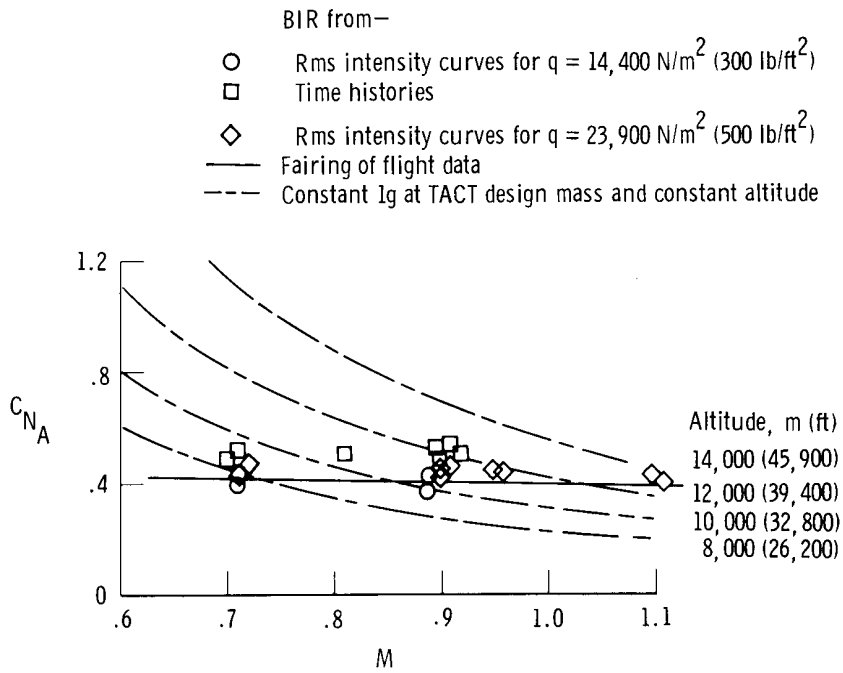


(c) TACT aircraft,  $\lambda = 35^\circ$ .

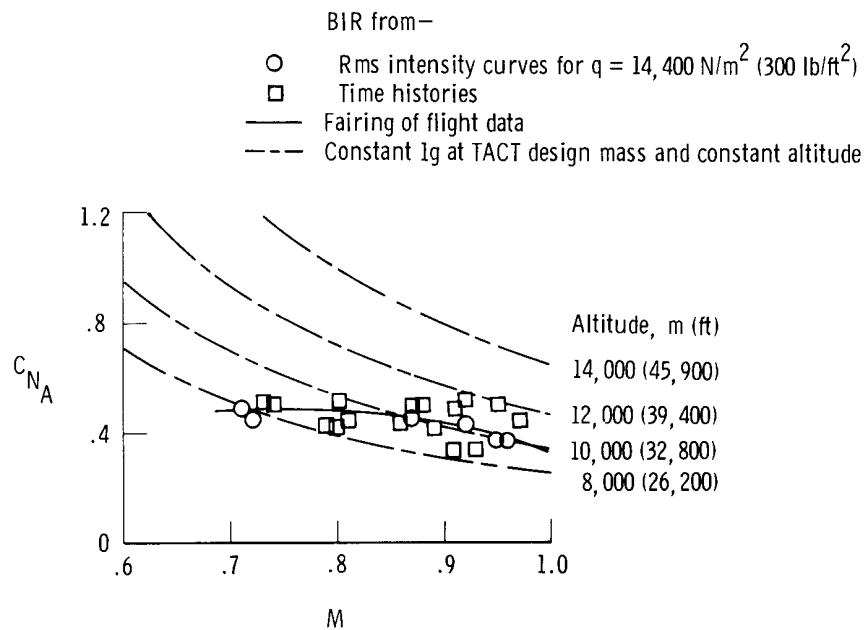


(d) Baseline aircraft,  $\lambda = 35^\circ$ .

Figure 6. Continued.

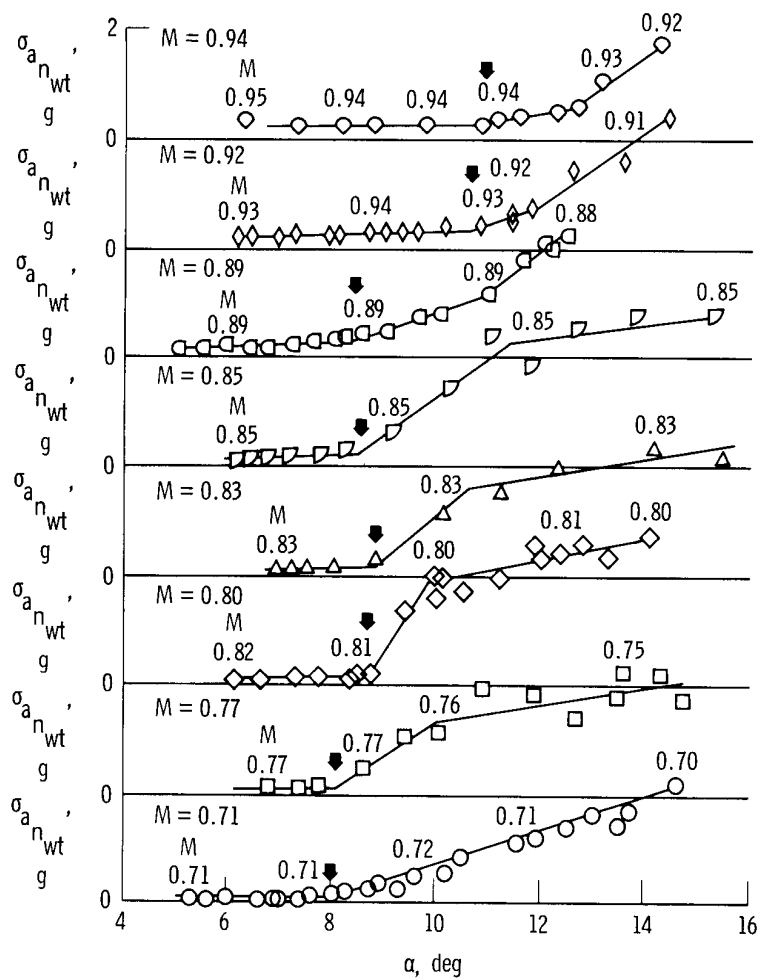


(e) TACT aircraft,  $\lambda = 58^\circ$ .



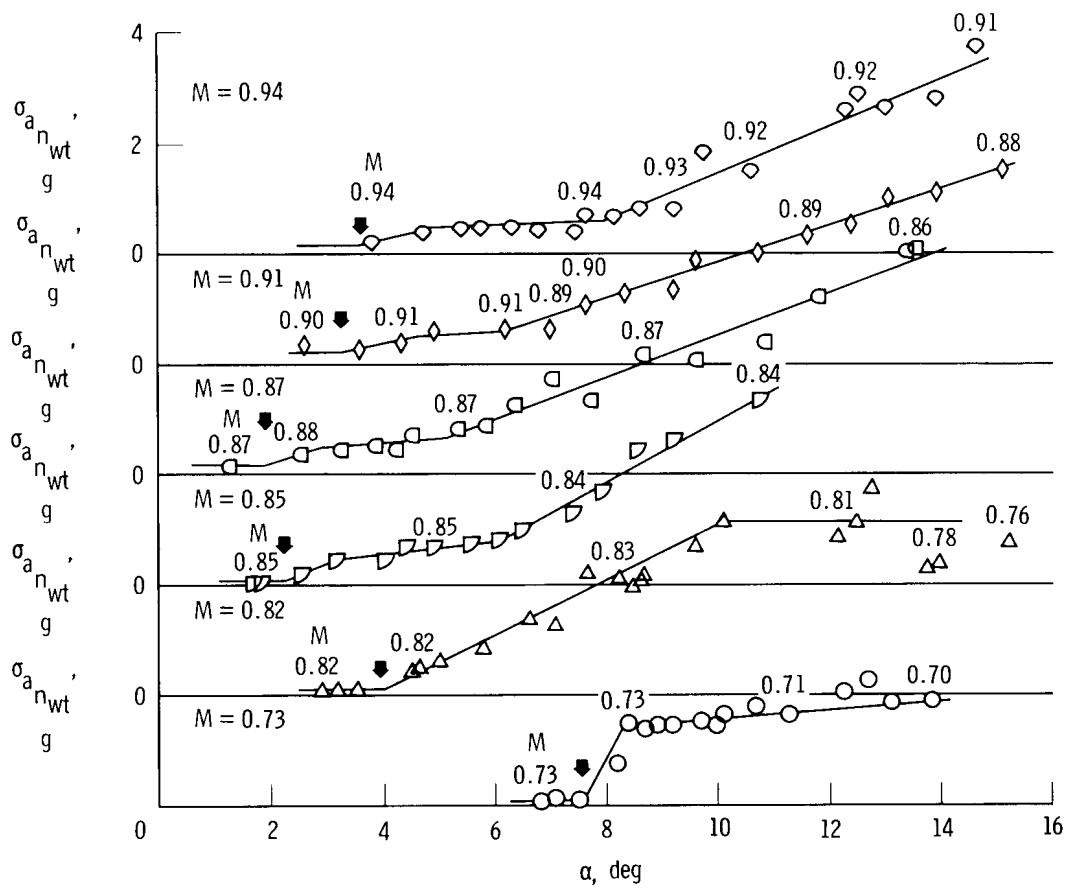
(f) Baseline aircraft,  $\lambda = 58^\circ$ .

Figure 6. Concluded.



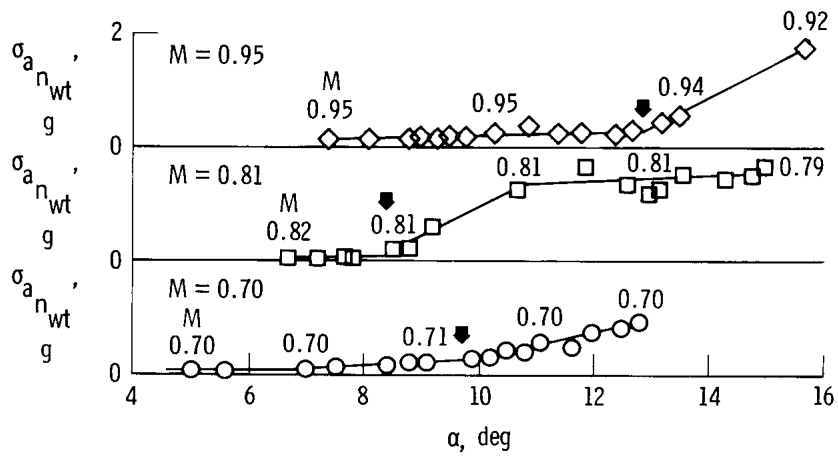
(a) TACT aircraft,  $\lambda = 26^\circ$ .

Figure 7. Buffet intensity curves. Arrows indicate BIR points.

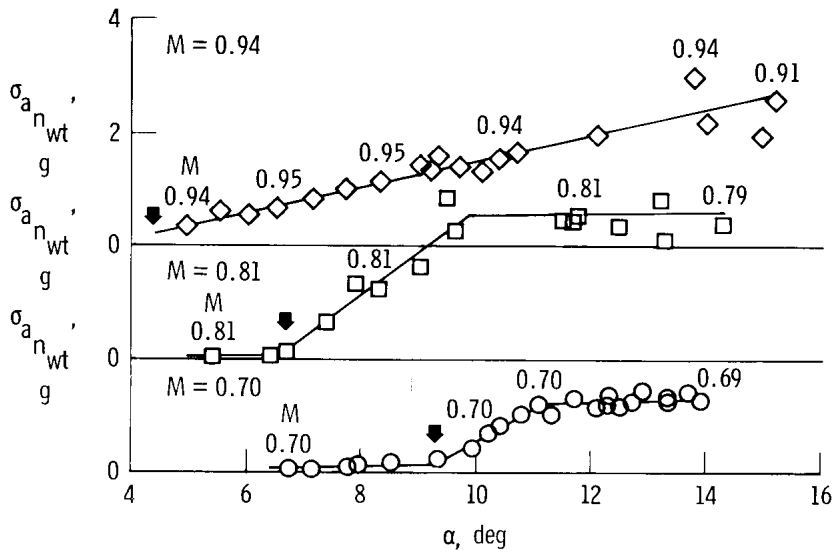


(b) Baseline aircraft,  $\lambda = 26^\circ$ .

Figure 7. Continued.

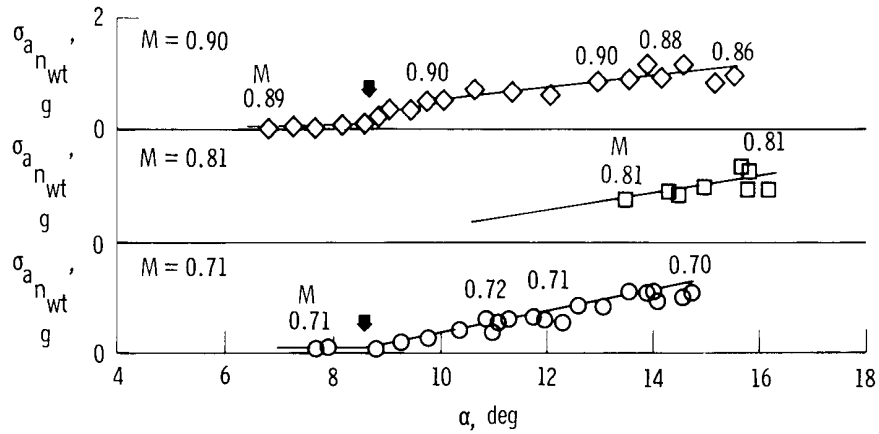


(c) TACT aircraft,  $\lambda = 35^\circ$ .

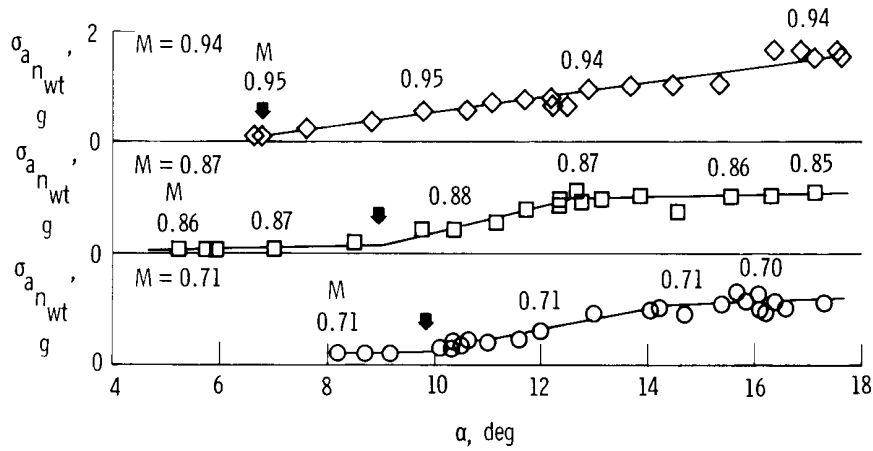


(d) Baseline aircraft,  $\lambda = 35^\circ$ .

Figure 7. Continued.

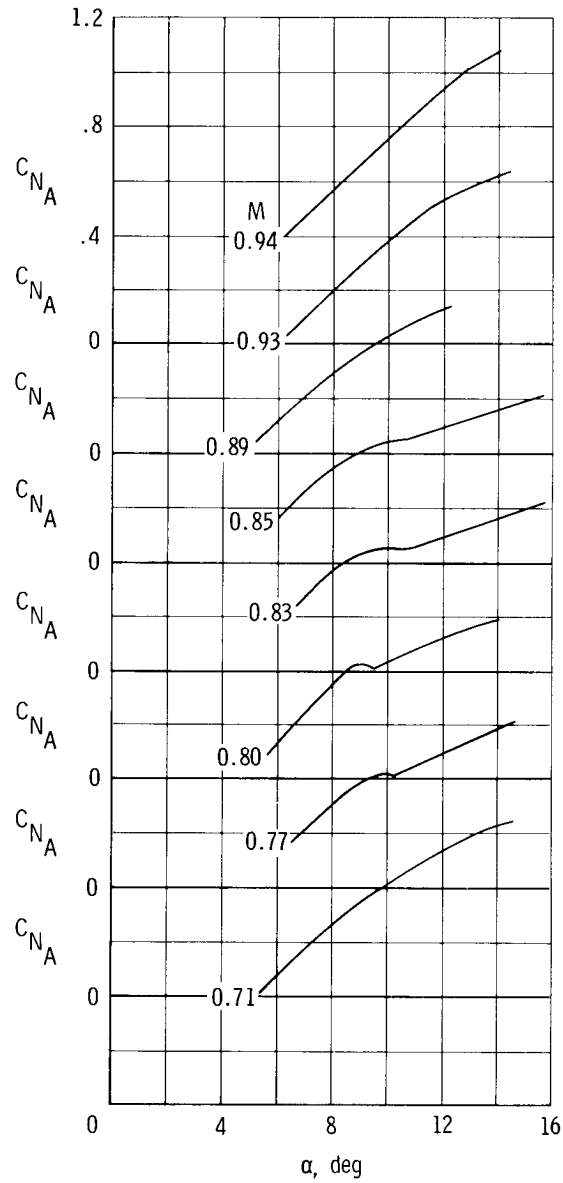


(e) TACT aircraft,  $\lambda = 58^\circ$ .



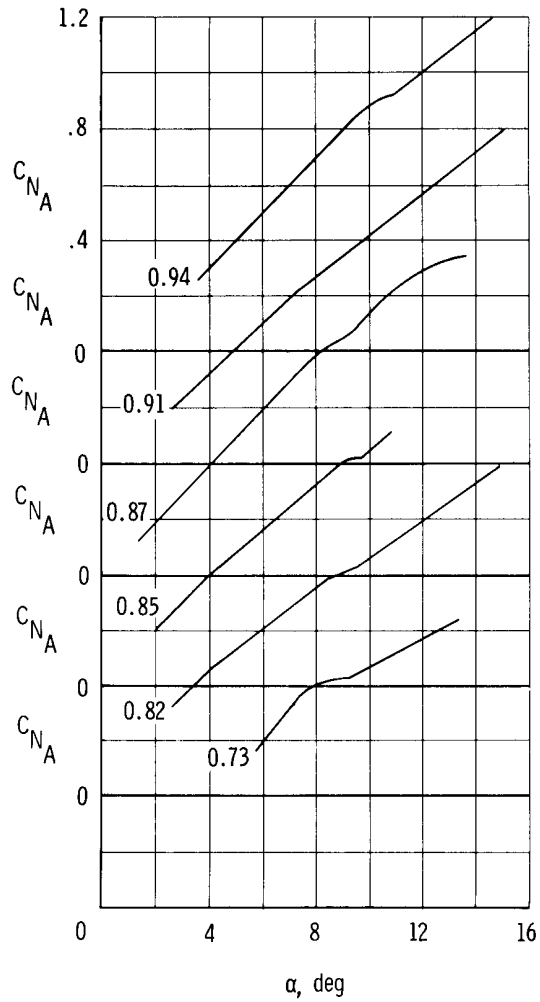
(f) Baseline aircraft,  $\lambda = 58^\circ$ .

Figure 7. Concluded.



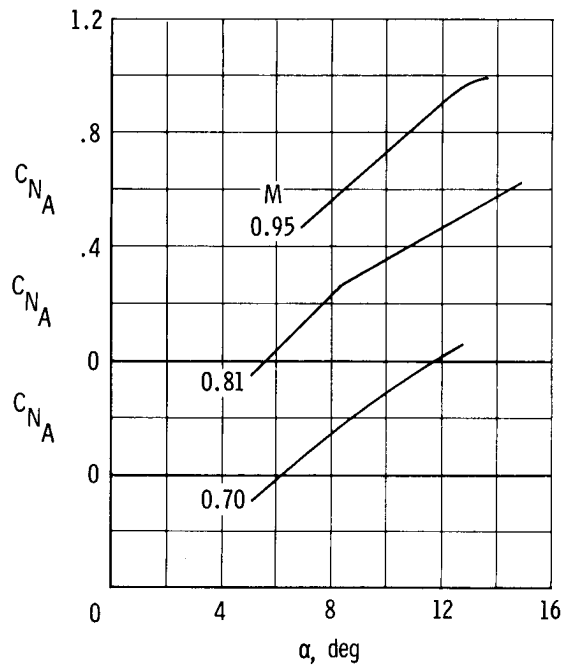
(a) TACT aircraft,  $\lambda = 26^\circ$ .

Figure 8. Variation of normal-force coefficient with angle of attack for data from figure 7.

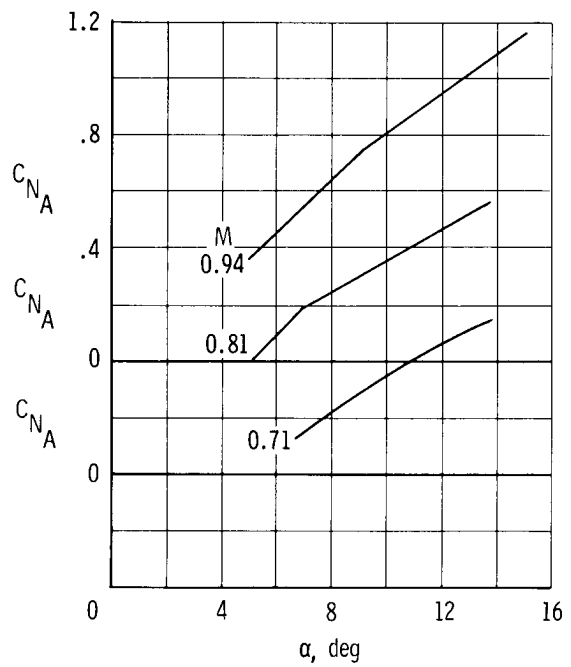


(b) Baseline aircraft,  $\lambda = 26^\circ$ .

Figure 8. Continued.

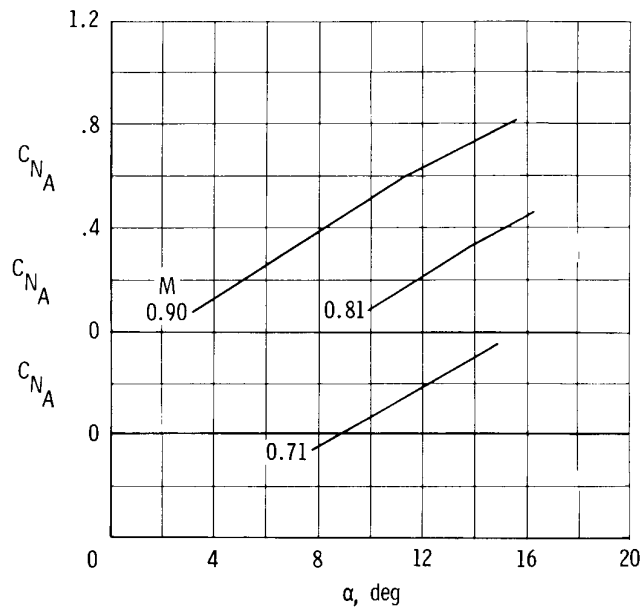


(c) TACT aircraft,  $\lambda = 35^\circ$ .

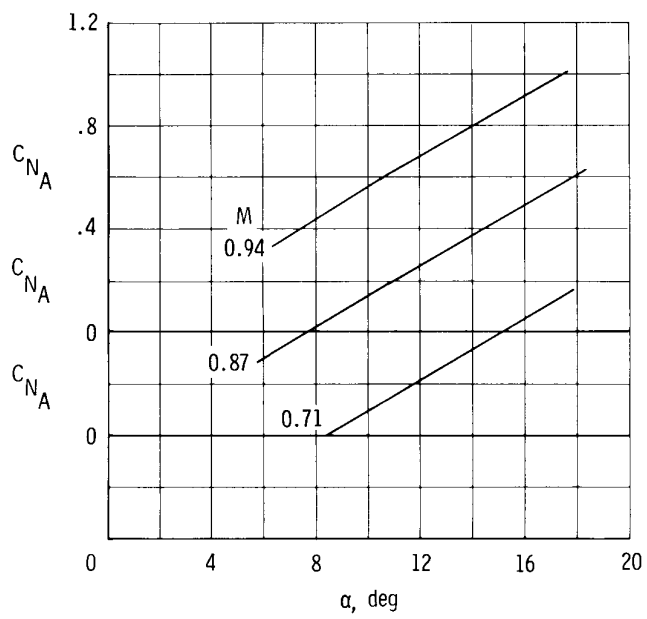


(d) Baseline aircraft,  $\lambda = 35^\circ$ .

Figure 8. Continued.

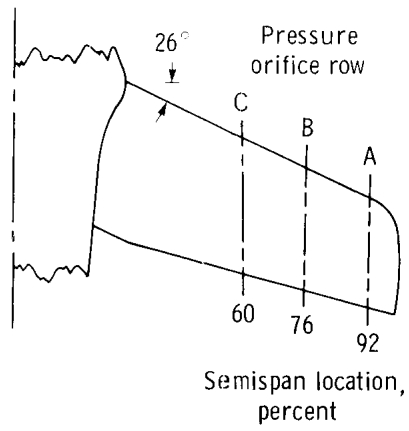


(e) TACT aircraft,  $\lambda = 58^\circ$ .

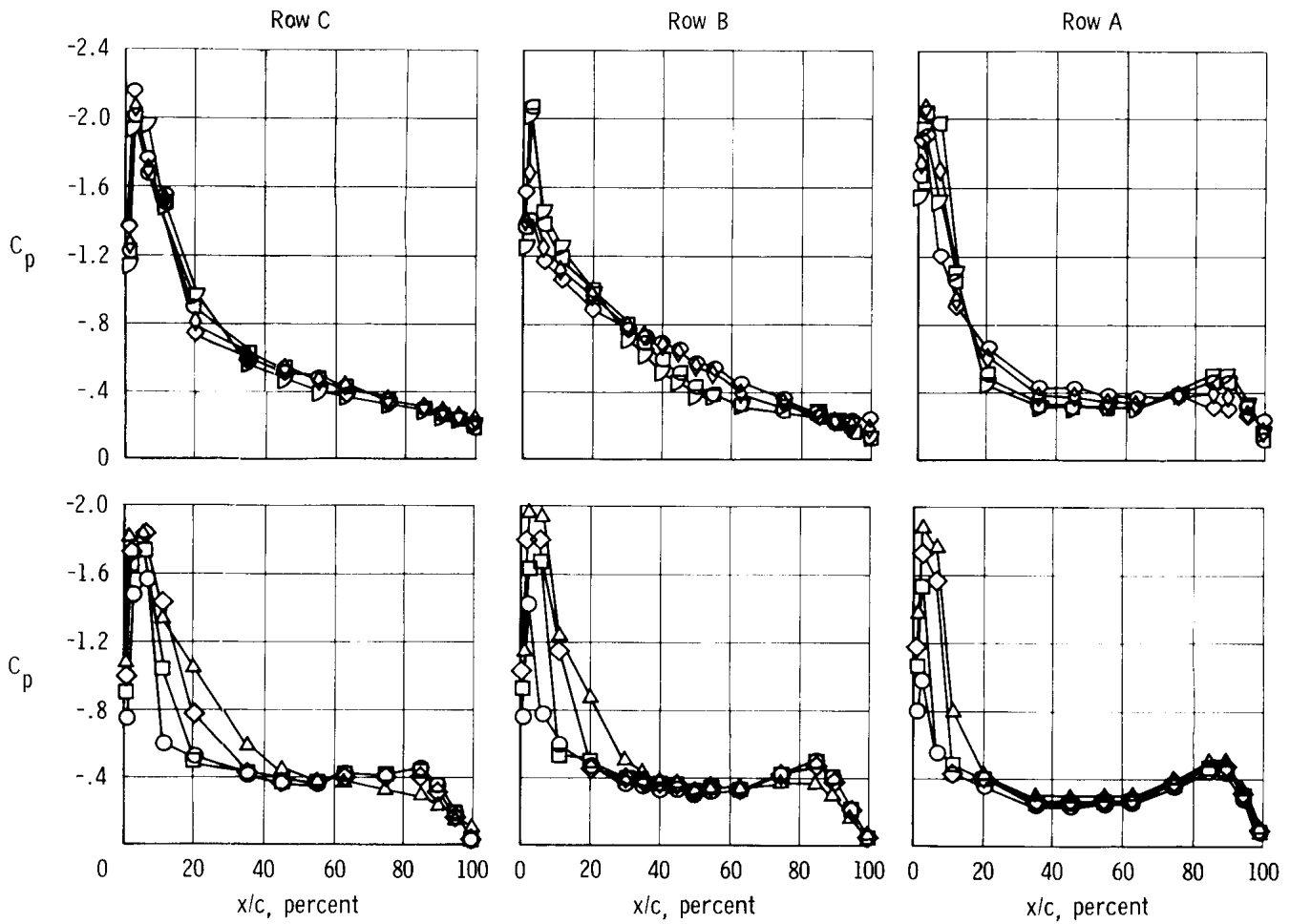


(f) Baseline aircraft,  $\lambda = 58^\circ$ .

Figure 8. Concluded.

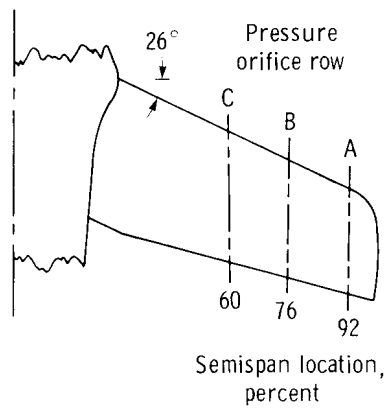


- $\alpha$ , deg
- 6
  - 7
  - ◇ 8
  - △ 9
  - ▽ 10
  - ◻ 11
  - ◊ 12
  - ◌ 13

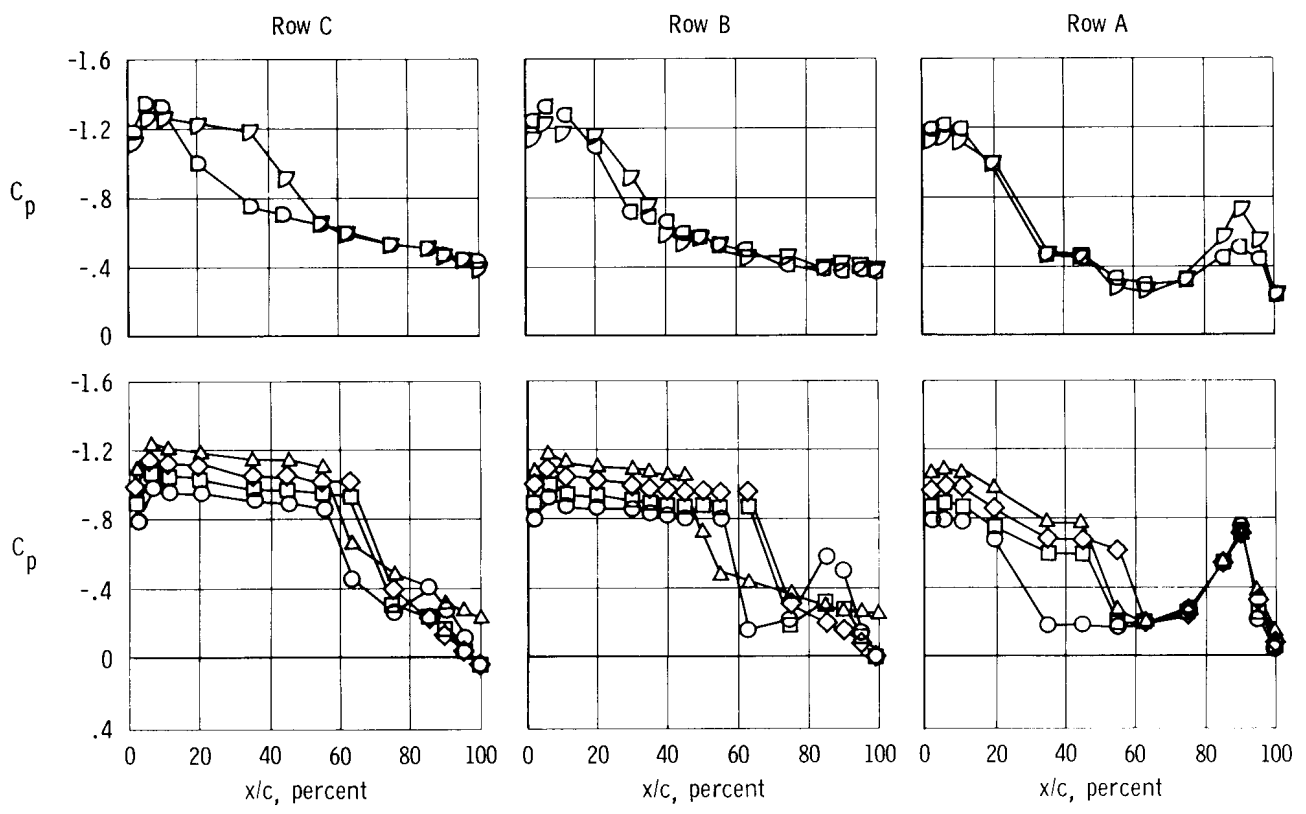


(a) Mach 0.70.

Figure 9. TACT flight-measured upper-surface pressure distributions.

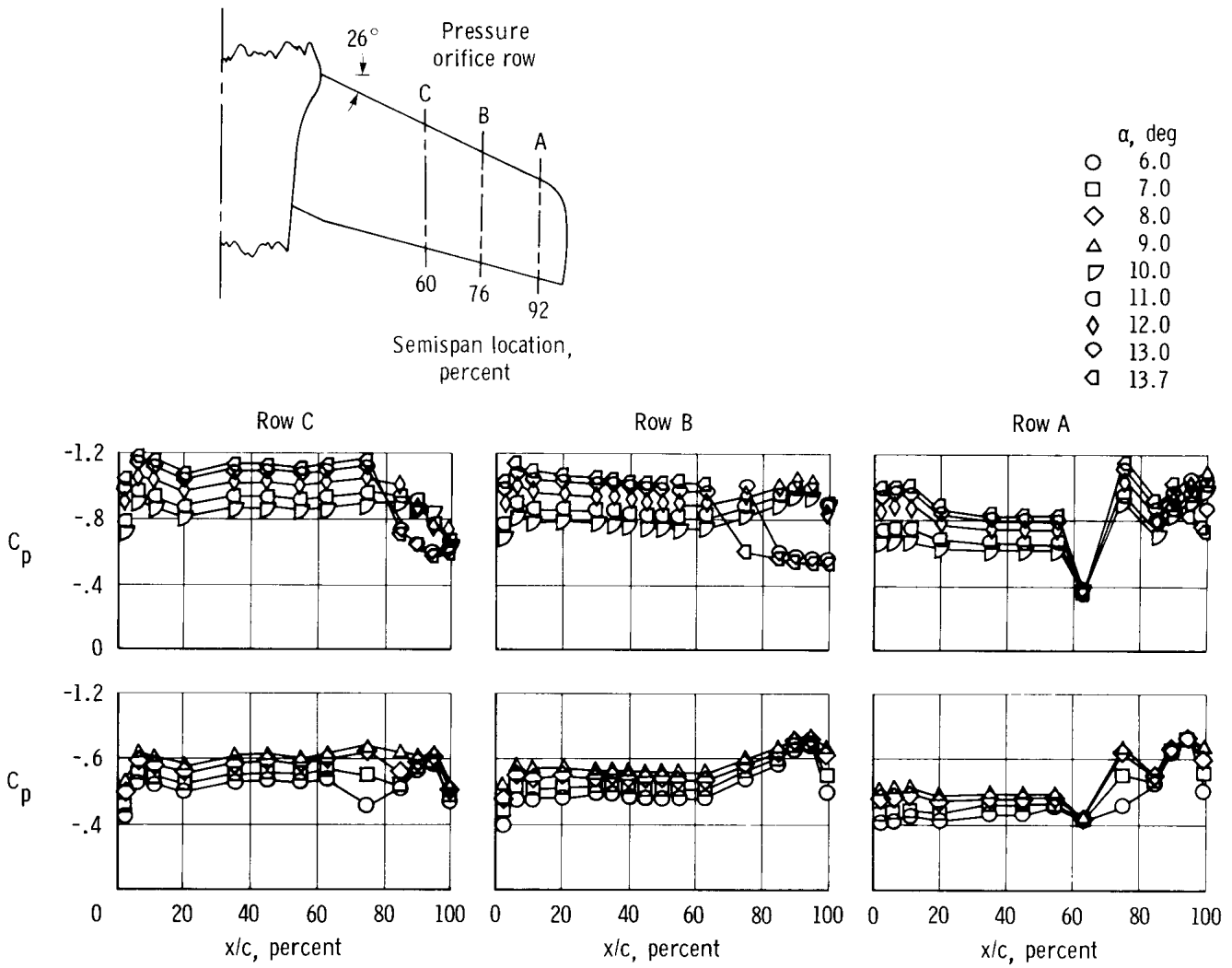


- $\alpha$ , deg
- 6
  - 7
  - ◇ 8
  - △ 9
  - ▽ 10
  - ◻ 11



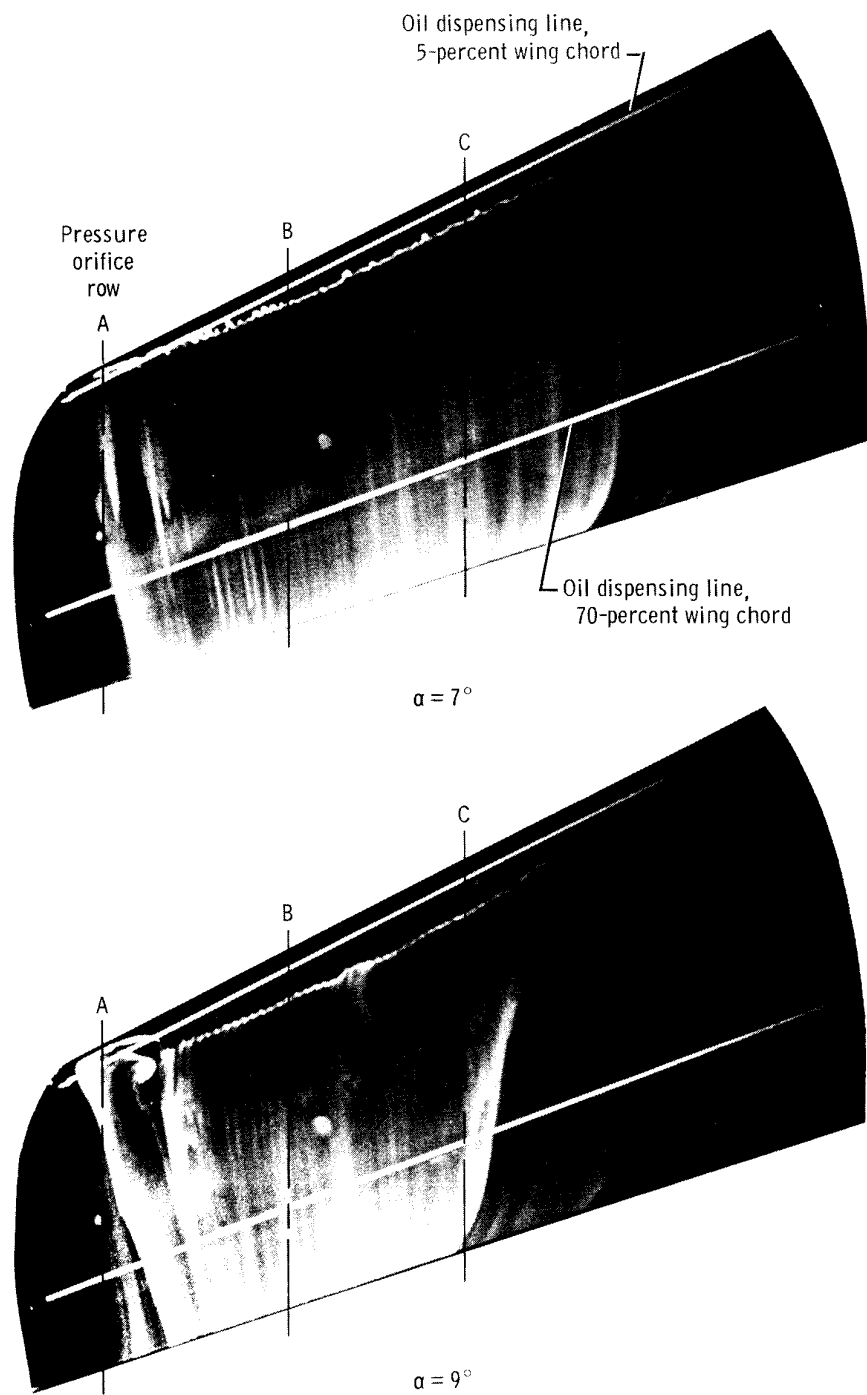
(b) Mach 0.85.

Figure 9. Continued.



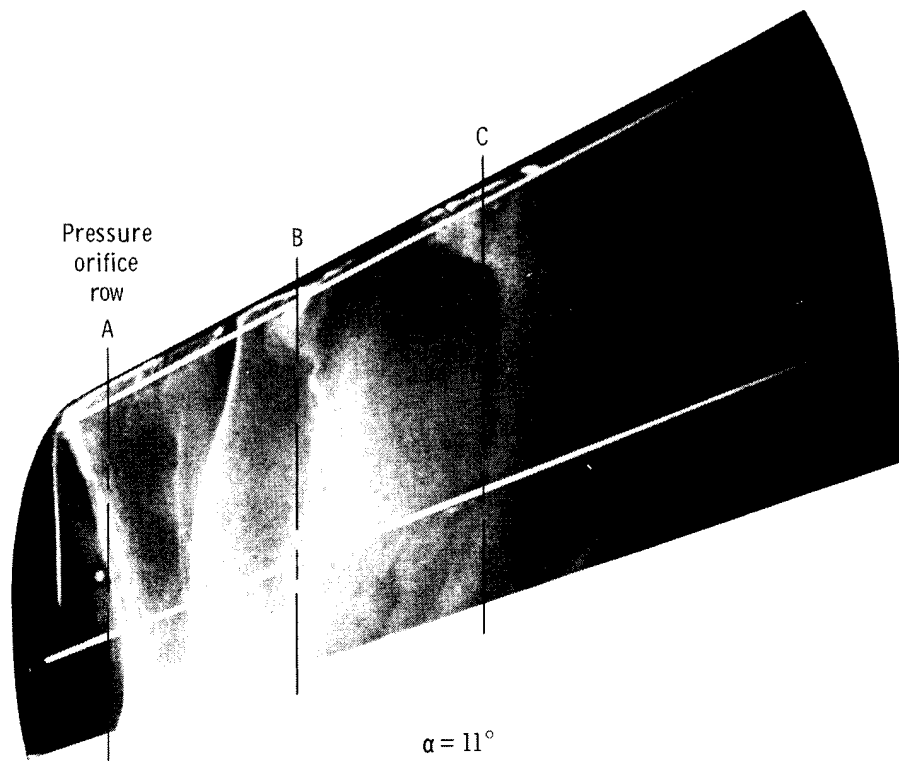
(c) Mach 0.95.

Figure 9. Concluded.



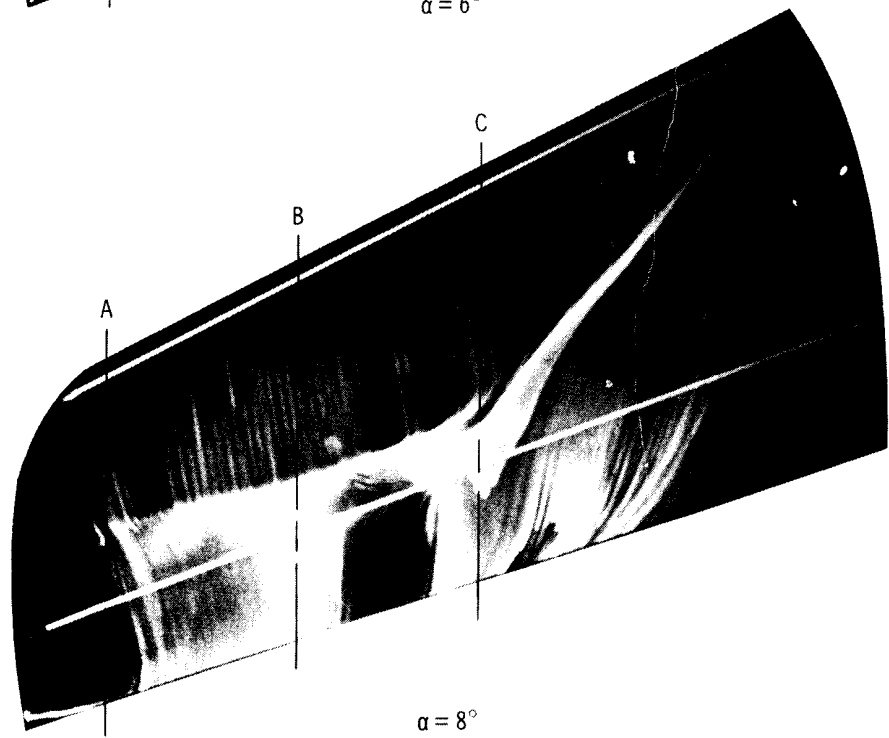
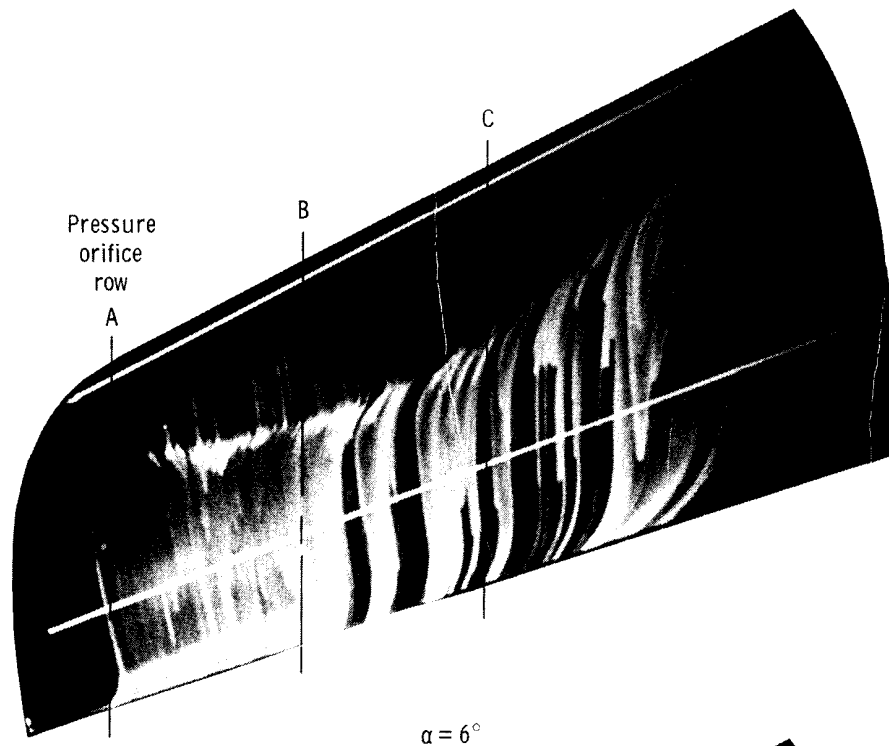
(a) Mach 0.70.

Figure 10. TACT wind tunnel upper-surface oil-flow photographs.  $\lambda = 26^\circ$ .



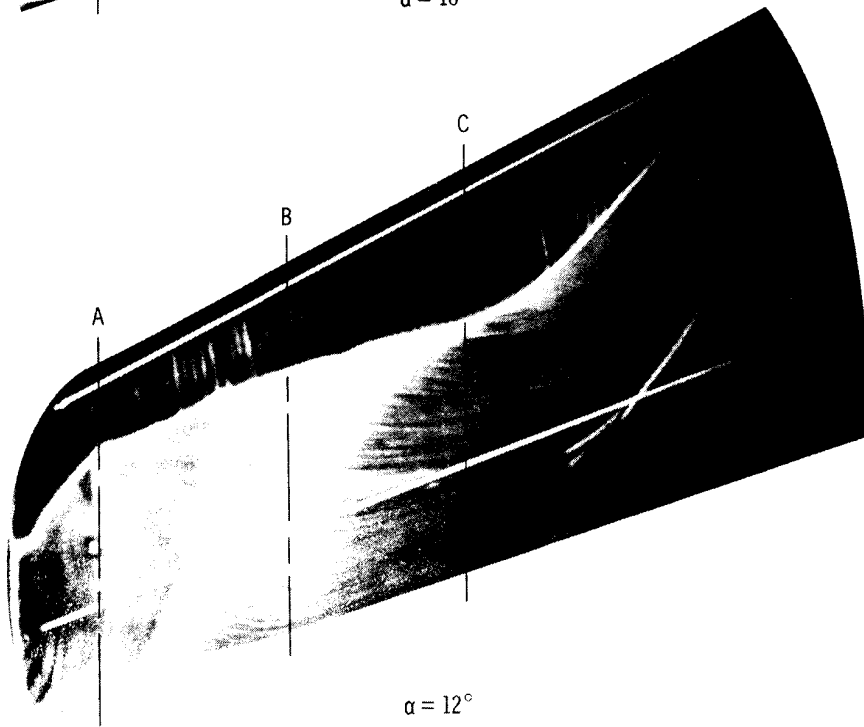
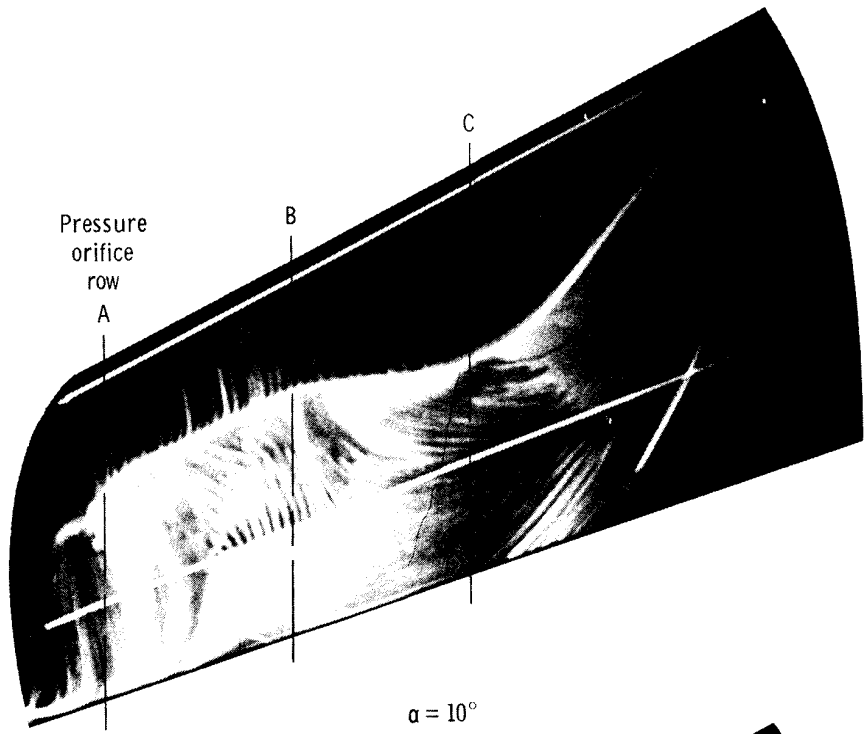
(a) Concluded.

Figure 10. Continued.



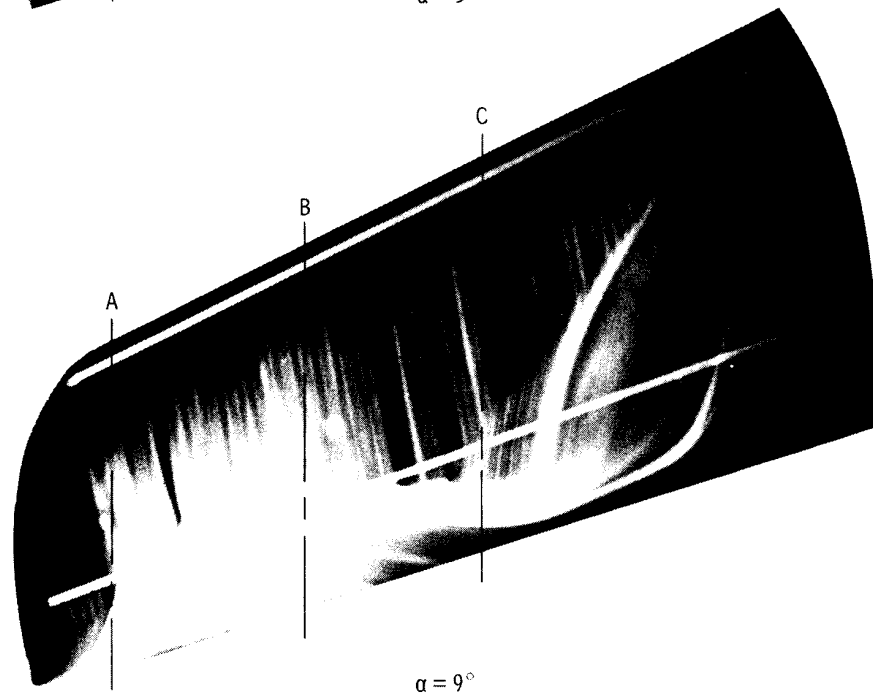
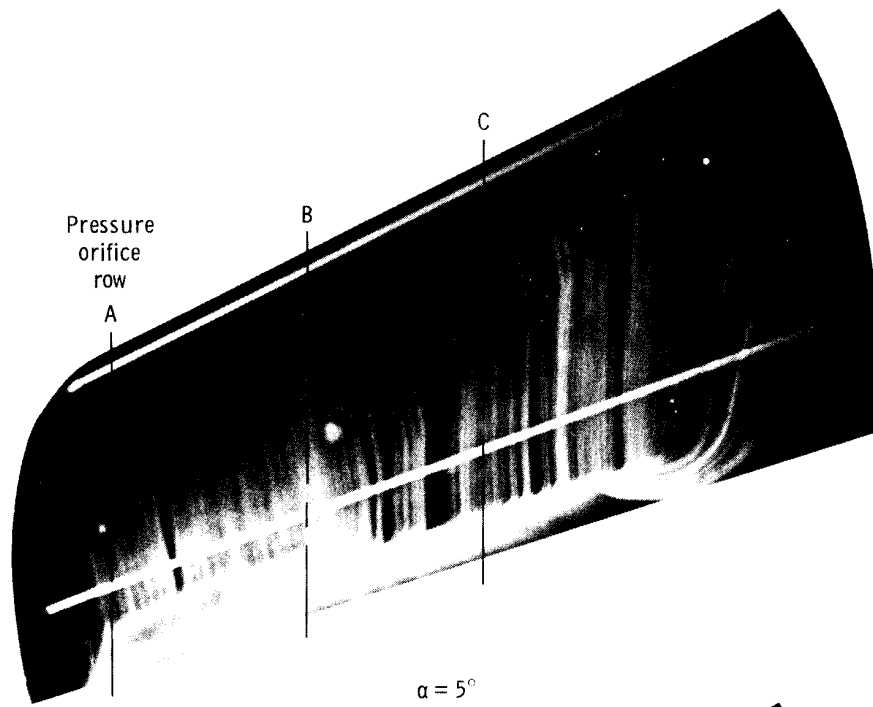
(b) Mach 0.85.

Figure 10. Continued.



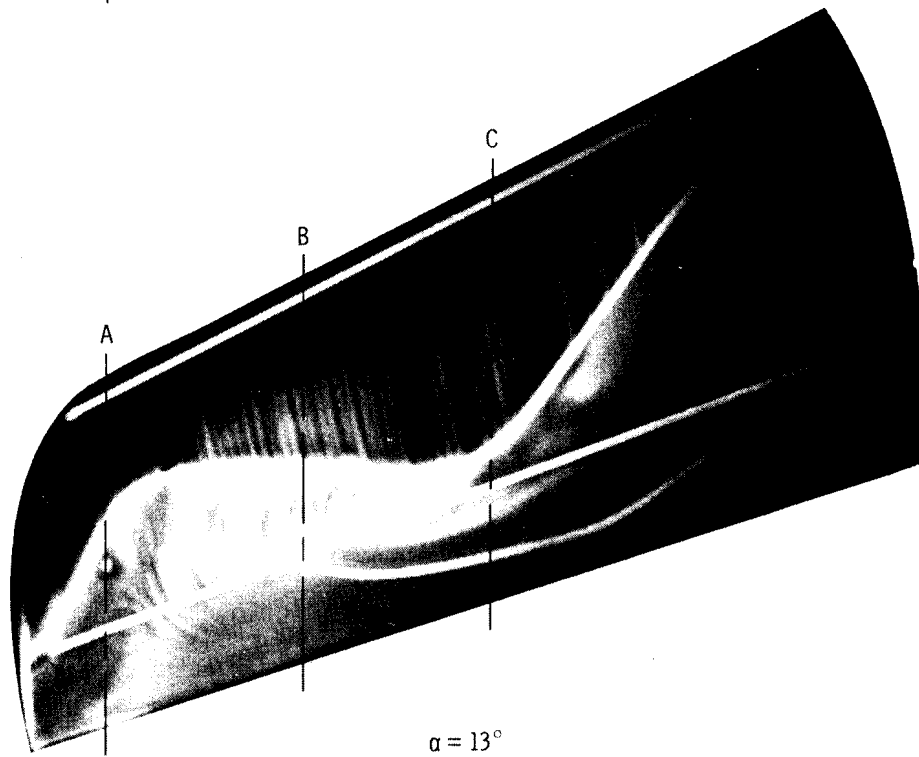
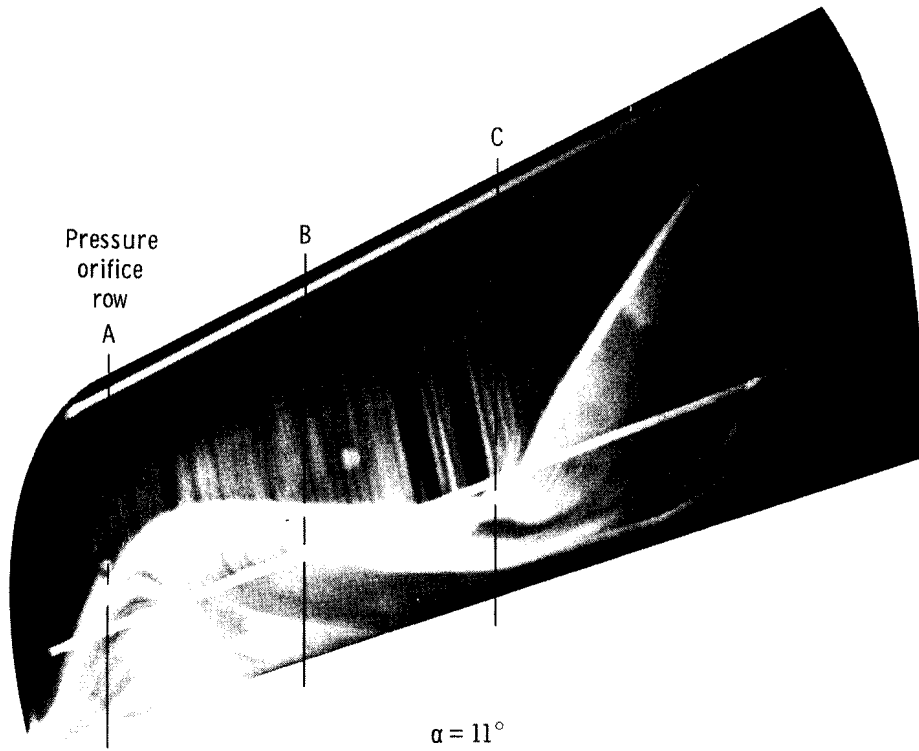
*(b) Concluded.*

*Figure 10. Continued.*



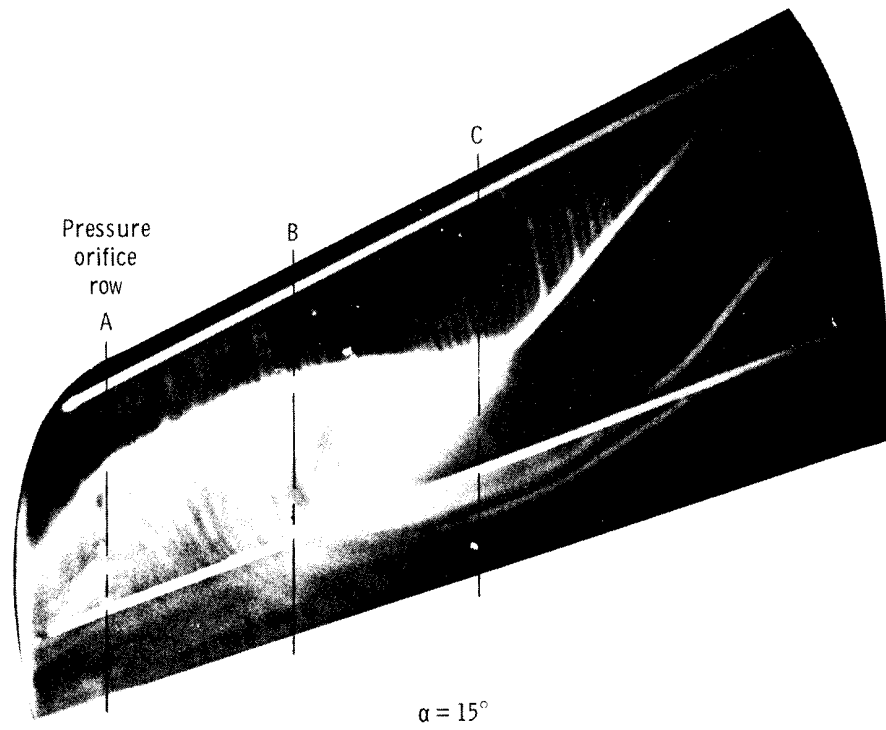
(c) Mach 0.95.

Figure 10. Continued.



(c) Continued.

Figure 10. Continued.



(c) *Concluded.*

*Figure 10. Concluded.*

|  |  |  |  |  |                      |
|--|--|--|--|--|----------------------|
| 1. Report No.<br>NASA TP-1244  |  | 2. Government Accession No.                          |  | 3. Recipient's Catalog No.                               |                      |
| 4. Title and Subtitle<br>FLIGHT-MEASURED BUFFET CHARACTERISTICS OF A<br>SUPERCRITICAL WING AND A CONVENTIONAL WING<br>ON A VARIABLE-SWEEP AIRPLANE   |  |  |  | 5. Report Date<br>May 1978                               |                      |
|  |  |  |  | 6. Performing Organization Code<br>H-991                 |                      |
| 7. Author(s)<br>Richard C. Monaghan  |  |  |  | 8. Performing Organization Report No.                    |                      |
| 9. Performing Organization Name and Address<br>NASA Dryden Flight Research Center<br>P.O. Box 273<br>Edwards, California 93523   |  |  |  | 10. Work Unit No.<br>505-11-24                           |                      |
|  |  |  |  | 11. Contract or Grant No.                                |                      |
| 12. Sponsoring Agency Name and Address<br>National Aeronautics and Space Administration<br>Washington, D.C. 20546  |  |  |  | 13. Type of Report and Period Covered<br>Technical Paper |                      |
|  |  |  |  | 14. Sponsoring Agency Code                               |                      |
| 15. Supplementary Notes  |  |  |  |  |                      |
| 16. Abstract   |  |  |  |  |                      |
| <p>Windup-turn maneuvers were performed to assess the buffet characteristics of the F-111A aircraft and the same aircraft with a supercritical wing, which is referred to as the F-111 transonic aircraft technology (TACT) aircraft. Data were gathered at wing sweep angles of 26°, 35°, and 58° for Mach numbers from 0.60 to 0.95. Wingtip accelerometer data were the primary source of buffet information. The analysis was supported by wing strain-gage and pressure data taken in flight, and by oil-flow photographs taken during tests of a wind tunnel model.</p> <p>Buffet intensity rise boundaries in the form of plots of airplane normal-force coefficient as a function of Mach number, as well as individual buffet intensity curves at specific Mach numbers are presented for each aircraft. In the transonic speed range, the overall buffet characteristics of the aircraft having a supercritical wing are significantly improved over those of the aircraft having a conventional wing. At subsonic speeds or at the aft wing sweep position where the supercritical wing is off design, the aircraft have similar buffet characteristics. Buffet intensity characteristics are interpreted from wing upper-surface pressure measurements and wind tunnel model oil-flow photographs.</p> |  |  |  |  |                      |
| 17. Key Words (Suggested by Author(s))<br>Transonic aircraft technology<br>Buffet<br>Supercritical wing<br>F-111 aircraft  |  |  | 18. Distribution Statement<br><br>Unclassified—Unlimited<br><br>Category: 02 |  |                      |
| 19. Security Classif. (of this report)<br>Unclassified   |  | 20. Security Classif. (of this page)<br>Unclassified |  | 21. No. of Pages<br>41                                   | 22. Price*<br>\$3.75 |

\*For sale by the National Technical Information Service, Springfield, Virginia 22161